Math. Model. Nat. Phenom. 20 (2025) 13
https://doi.org/10.1051/mmnp/2025004

Mathematical Modelling of Natural Phenomena
www.mmnp-journal.org

ENHANCING MAXIMUM SUSTAINABLE YIELD IN A MULTI-PATCH ROSENZWEIG–MACARTHUR MODEL WITH SYMMETRICAL PREY AND ASYMMETRICAL PREDATOR MIGRATION

Ali Moussaoui[1,*], Pierre Auger[2] and Bilel Elbetch[3]

Abstract. In this paper, we formulate a Rosenzweig–MacArthur (RM) predator–prey model incorporating the dispersal of both prey and predator among n discrete habitat patches. We assume that only the predator is harvested and not its prey, growing logistically on each site. Our aim is to investigate whether the total catch in a system of interconnected patches through migration can surpass the sum of the optimal catch from n isolated patches, known as the maximum sustainable yield (MSY). We start by revisiting some fundamental properties of the RM model examining the stability of its equilibrium points. We then analyze the MSY for a single patch, deriving conditions on the fishing effort required to achieve MSY. Next, we consider the MSY of the RM model for both separated and connected patches, and provide different answers to the aforementioned question for different cases. In the homogeneous case with symmetric movement of the prey between patches, we show that the total yield at MSY for the interconnected system is equivalent to the sum of the yields at MSY for each isolated patch. In contrast, in the heterogeneous case, we show that the total maximum sustainable yield for the connected patches can surpass the sum of the maximum sustainable yields for each isolated patch. Our analysis establishes the conditions under which one scenario is more favorable in terms of yield.

Mathematics Subject Classification. 37N25, 92D25, 34D23, 34D15.

Received July 23, 2024. Accepted January 20, 2025.

1. Introduction

In the fields of science and engineering, many complex systems can be accurately represented using networks of interconnected differential equations. Mathematically, such a network is represented as a weighted directed graph (digraph), comprising n vertices and a series of directed arcs. The specific class of dynamical systems

Keywords and phrases: Maximum sustainable yields, resource management, predator–prey model, Schaefer model, slow–fast systems, Tikhonov's theorem.

[1] Laboratory of Nonlinear Analysis and Applied Mathematics, Department of Mathematics, Faculty of Science, University of Tlemcen, 13000, Algeria.
[2] UMMISCO, Sorbonne Université, Institut de Recherche pour le Développement, IRD, 93143 Bondy, France.
[3] Faculty of Mathematics, University of Sciences and Technology Houari Boumediene, Algiers, Algeria.

* Corresponding author: moussaouidz@yahoo.fr

explored in this context is generally formulated as follows:

$$\frac{\mathrm{d}x}{\mathrm{d}t} = f(x) + \epsilon\Gamma x,$$

where $f(x)$ characterizes the system's dynamics in the absence of interaction which depends on the state variables x. The term $\epsilon\Gamma x$ captures the impact of interconnections between different nodes, with ϵ indicating the migration rate and Γ being the migration matrix that quantifies exchanges between the nodes. This model, referred to as the complete system, integrates multiple subsystems through coupling. A notable scenario within these systems is that of perfect mixing, which occurs when the migration rate ϵ goes to infinity, in other words, when there is no restriction whatsoever on travel (for further details and examples, see [1–7]). A critical ecological question arises in this context: is it possible, depending on the migration rate, that the total equilibrium population be larger than the sum of the carrying capacities $\sum_i K_i$? This question is pivotal in determining whether migration enhances or diminishes the total equilibrium population. Extensive research has been devoted to this topic, examining various models and conditions under which dispersal is either beneficial or harmful. For further reading on logistic models, refer to [1, 2, 4, 6, 8–16]; for source-sink models, see [5, 17, 18]; for generalized growth rates, consult [3, 7]; for studies on susceptible-infected-susceptible (SIS) patch models, see [19–21]; and for research on populations with time-varying growth rates in sink environments and the phenomenon of dispersal-induced growth (DIG), see [22–24].

Recent mathematical models increasingly incorporate the spatial distribution of fisheries to study the management of multi-patch fisheries [25–30]. The concept of Maximum Sustainable Yield (MSY), which aims to maximize catches while ensuring the long-term sustainability of fish populations, is central to fisheries management strategies [31, 50, 53]. Calculating this yield is crucial for optimizing fishery productivity while ensuring the population remains viable. For a simplified approach to understanding how to calculate MSY in predator–prey models, see Section 2.

Auger *et al.* [8] studied the system of two fishing sites connected by fish migrations. They considered a Lotka-Volterra (LV) prey-predator model with a type I functional response with one fish species being preyed upon by a larger fish. In this work only the predator was fished on the two sites. They showed that the optimal catch of the predator at the MSY when the two sites are connected could be greater than the sum of the captures at the MSY of the two isolated sites. In other words, site connectivity can increase the total catch. More recently, Nguyen Ngoc *et al.* [32] studied into more details the LV prey predator model with asymmetric migrations of the prey and the predator. In this work, the heterogeneity parameters allowing to increase the MSY by connectivity have been clearly identified as well as their quantitative impact on the increase of MSY.

The case of the Rosenzweig-MacArthur (RM) model [51, 52] with a type II functional response with asymmetric migrations of the prey and the predator was already addressed in the article Auger *et al.* [8] still for a system of two connected fishing sites. Let us recall the RM model with two fishing sites studied in [8]. The complete RM model reads as follows:

$$\begin{cases} \dfrac{\mathrm{d}x_1}{\mathrm{d}t} = r_1 x_1\left(1-\dfrac{x_1}{K_1}\right) - \dfrac{a x_1 y_1}{x_1+D} + \epsilon(\gamma_2 x_2 - \gamma_1 x_1), \\ \dfrac{\mathrm{d}x_2}{\mathrm{d}t} = r_2 x_2\left(1-\dfrac{x_2}{K_2}\right) - \dfrac{a x_2 y_2}{x_2+D} + \epsilon(\gamma_1 x_1 - \gamma_2 x_2), \\ \dfrac{\mathrm{d}y_1}{\mathrm{d}t} = \left(\dfrac{e a x_1}{x_1+D} - d_1\right) y_1 - E_1 y_1 + \epsilon(\theta_2 y_2 - \theta_1 y_1), \\ \dfrac{\mathrm{d}y_2}{\mathrm{d}t} = \left(\dfrac{e a x_2}{x_2+D} - d_2\right) y_2 - E_2 y_2 + \epsilon(\theta_1 y_1 - \theta_2 y_2), \end{cases} \tag{1.1}$$

where x_i and y_i for $i = 1, 2$ denote the densities of preys and predators on the patch i, respectively. Parameters r_i and K_i represent the fish prey intrinsic growth rate and carrying capacity respectively on patch i. The fish predator catches the fish prey in 2 patches. Parameter a is the predation parameter in patch 1 and 2, e is the

conversion parameter of prey biomass into predator biomass and D is the predator mortality rate in patch 1 and 2. The predator is harvested in 2 patches at a fishing effort E_i. Parameters ϵ is the diffusion rate of prey and predator.

Taking advantage of the time scales, the complete model can be reduced into an aggregated model governing the evolution of total prey and predator biomass at the slow time scale. However, this aggregated model cannot be put in the form of the classic RM model. The reduced model remains different from local models because it includes in the prey equation two predation terms associated with each site which cannot be reduced to a single term to return to the classic RM model. Under these conditions, Auger *et al.* [8] carried out a bifurcation analysis to study the dynamics of this new aggregated model. Mention that they had already made some numerical examples showing that the total catch at MSY can be increased by connectivity of heterogeneous sites for the RM model.

The aggregated model takes the form of the RM model only in the case of a homogeneous spatial distribution of the prey *i.e.* for a symmetric migration matrix of the prey. This is the reason why in the present work, the study is limited to the case of a symmetric migration of the prey but with an asymmetric migration of the predator. The assumption of symmetric prey migration can be realistic especially if all the sites have the same carrying capacity. Indeed, it is known that prey fish tend to distribute themselves spatially according to the resource available on each site at the Ideal Free Distribution (IFD), *i.e.* proportionally to the local carrying capacity. If all sites have the same carrying capacity, it makes sense to assume a homogeneous distribution of fish. Heterogeneity of sites can nevertheless exist, particularly in terms of growth rates or even predation rates which can differ from one site to another. However, this work generalizes the study to the case of any number of sites greater than two in the case of the RM model with harvesting of the predator. At that stage we need to recall that Bravo de la Parra *et al.* [33] had already generalized the increase in MSY by connectivity to any number of sites not for the RM model but within the framework of the Gordon-Schaefer model.

The paper is organized as follows. In Section 2, we revisit some fundamental properties of the Rosenzweig-MacArthur model and examine the stability of its equilibrium points. Subsequently, we analyze the MSY for a single patch, deriving the conditions on fishing effort required to achieve this yield. Section 3 extends the model to include spatial distribution by considering a network of n patches. Here, we explore how the spatial structure and interactions between patches influence the overall dynamics of the predator–prey system. In Section 4, we investigate the model's behavior as the migration rate approaches infinity using singular perturbation arguments and Tikhonov's theorem [34, 35]. In Section 5, we show that, when the migration rate goes to infinity, the MSY for the connected patches can exceed the sum of the catches on each isolated patch. This analysis enables us to establish the conditions under which one scenario is more advantageous in terms of yield, and we provide a comprehensive classification of all possible cases. Section 6 is dedicated to numerical simulations that illustrate the theoretical findings from the previous sections. The final section contains concluding remarks. Some mathematical details are provided in the Appendix.

2. The Rosenzweig-Macarthur predator–prey model and Maximum Sustainable Yield

In this part, we consider the predator- prey model with a Holling type II functional response with constant harvesting:

$$\begin{cases} \dfrac{\mathrm{d}x}{\mathrm{d}t} = rx\left(1-\dfrac{x}{K}\right) - \dfrac{axy}{x+D}, \\ \dfrac{\mathrm{d}y}{\mathrm{d}t} = \left(e\dfrac{ax}{x+D} - d\right)y - Ey. \end{cases} \tag{2.1}$$

where x is the prey (resource) biomass and y the predator biomass at time t. In this model, the resource grows logistically with growth rate r and carrying capacity K. The predator feeds from the resource and is harvested at a constant rate (fishing effort) E. Parameters a and D are the predation parameters and e the conversion

efficiency of the prey biomass into predator biomass. Parameter d is the natural death rate of the predator. The dynamics of the system (2.1) is well studied (*e.g.*, see [36] and [37]). In this section, we provide a succinct overview of the stability of equilibrium of this system. The coexisting equilibrium of the unexploited system (2.1) (where $E = 0$) is found at the intersection of the nontrivial prey isocline at equilibrium, given by

$$y = \frac{r}{a}(x + D)\left(1 - \frac{x}{K}\right)$$

and the nontrivial predator isocline at equilibrium, expressed as

$$e\frac{ax}{x + D} = d$$

within the positive quadrant.

Naturally, the predator isocline is a simple straight line parallel to the predator axis. Additionally, the prey biomass at equilibrium, denoted as

$$x^* = \frac{dD}{ea - d}$$

(provided $ea > d$) is entirely determined by the parameters related to predator growth, assuming $ea > d$. Conversely, the prey isocline is a quadratic function of x and reaches its maximum at

$$x = x^M = \frac{K - D}{2}$$

If the prey biomass x^* at the coexisting equilibrium exceeds x^M, both species experience globally stable coexistence [38]. Otherwise, the system shows a globally stable limit cycle [38–40].
The conditions for the existence and positivity of the equilibrium points of the model of RM can also be restated as follows:

- If $ea\frac{K-D}{K+D} \leq \mathrm{d} \leq ea\frac{K}{K+D}$, then (x^*, y^*) is globally asymptotically stable in the positive quadrant [41].
- If $\mathrm{d} \leq ea\frac{K-D}{K+D}$, then (x^*, y^*) is unstable and each orbit in the positive quadrant except the positive equilibrium converges to a periodic orbit. It is also known that the periodic orbit is unique [41].
- If $ea\frac{K}{K+D} < d$, the predator goes extinct, the positive equilibrium does not exist in the in the nonnegative quadrant and $(K, 0)$ is globally asymptotically stable.

Without any loss of generality and assuming no harvesting, we consider that both species coexist in the form of oscillations (*i.e.*, $x^* < x^M$). As the effort E increases, x^M remains fixed, but

$$x^*(E) = \frac{D(d + E)}{ea - d - E}$$

shifts to the right on the prey axis x. Thus, increasing the harvesting effort on the predator species can eliminate these oscillations. A sufficiently large effort can ensure that $x^M < x^*(E)$, resulting in stable coexistence in the RM model.

Since a sufficiently large effort on predator species can lead to stable coexistence, one might wonder if the effort at the Maximum Sustainable Yield (MSY) is large enough to achieve this stability. To explore this, we examine whether predator stock levels at MSY harvesting correspond to a stable equilibrium. The coexisting equilibrium for predator harvesting is given by

$$(x^*(E), y^*(E)) = \left(\frac{D(d + E)}{ea - d - E}, \frac{rD}{a}\left(1 + \frac{d + E}{ea - d - E}\right)\left(1 - \frac{D(d + E)}{K(ea - d - E)}\right)\right).$$

Assuming that and $d+E<ea\frac{K}{K+D}$, the coexisting equilibrium $(x^*(E);y^*(E))$ belongs to the positive cone in the phase plane. The total harvesting yield $Y^*(E):=Ey^*(E)$ reads:

$$Y^*(E)=\begin{cases}\dfrac{rDE}{a}\left(1+\dfrac{d+E}{ea-d-E}\right)\left(1-\dfrac{D(d+E)}{K(ea-d-E)}\right) & if \quad E<\dfrac{K(ea-d)-dD}{K+D},\\ 0 & else.\end{cases} \tag{2.2}$$

and it would be the maximum when

$$E^*_{MSY}=\frac{(ea-d)[K(ea-d)-dD]}{K(ea-d)-dD+2eaD} \tag{2.3}$$

with the prey biomass

$$x^*_{MSY}=\frac{K}{2}+\frac{dD}{2(ea-d)} \tag{2.4}$$

and the yield at MSY:

$$Y^*_{MSY}=\frac{r}{4aK}\frac{(K(ea-d)-dD)^2}{ea-d}. \tag{2.5}$$

Since $x^M<x^*_{MSY}$, the predator stock at MSY experiences a stable coexistence. Figure 1 illustrates various aspects of a predation model based on the specified parameters ($r=3, K=10, a=2, e=0.75, D=4, d=0.5$). It shows the evolution of the maximum real part of the eigenvalues relative to the effort applied to the predator, with blue indicating stable equilibrium and red indicating unstable equilibrium. Additionally, the figure depicts the variation in total prey and predator densities and includes a yield curve that reaches its maximum at the stable state. This comprehensive figure facilitates the analysis of how population dynamics and ecosystem stability are influenced by the management effort applied to predators.

3. Multi-patch Holling type II predator–prey model

Patchy predator–prey models can be used to model complex ecosystems of predator–prey interactions in a heterogeneous environment. Assume that prey and predator populations interact in each patch with a Holling type II functional response at each patch and can disperse among patches. Then we obtain the following predator–prey model in which prey and predator move among n patches ($n\geq 2$)

$$\begin{cases}\dfrac{\mathrm{d}x_i}{\mathrm{d}t}=r_ix_i\left(1-\dfrac{x_i}{K_i}\right)-\dfrac{a_ix_iy_i}{x_i+D_i}+\epsilon\displaystyle\sum_{j=1,j\neq i}^{n}(\gamma_{ij}x_j-\gamma_{ji}x_i),\\ \dfrac{\mathrm{d}y_i}{\mathrm{d}t}=\left(\dfrac{ea_ix_i}{x_i+D_i}-d_i\right)y_i-E_iy_i+\epsilon\displaystyle\sum_{j=1,j\neq i}^{n}(\theta_{ij}y_j-\theta_{ji}y_i),\end{cases} \quad i=1,\cdots,n. \tag{3.1}$$

Here, x_i and y_i denote the densities of preys and predators on the patch i, respectively. Parameters r_i and K_i represent the fish prey intrinsic growth rate and carrying capacity respectively on patch i. The fish predator catches the fish prey in n patches. Parameter a_i is the predation parameter in patch i, e is the conversion parameter of prey biomass into predator biomass and d_i is the predator mortality rate in patch i. The predator is harvested in n patches at a fishing effort E_i. Parameters ϵ is the diffusion rate of prey and predator. The term on the right hand side of the system (3.1) describes the effect of the linear migration between the n patches,

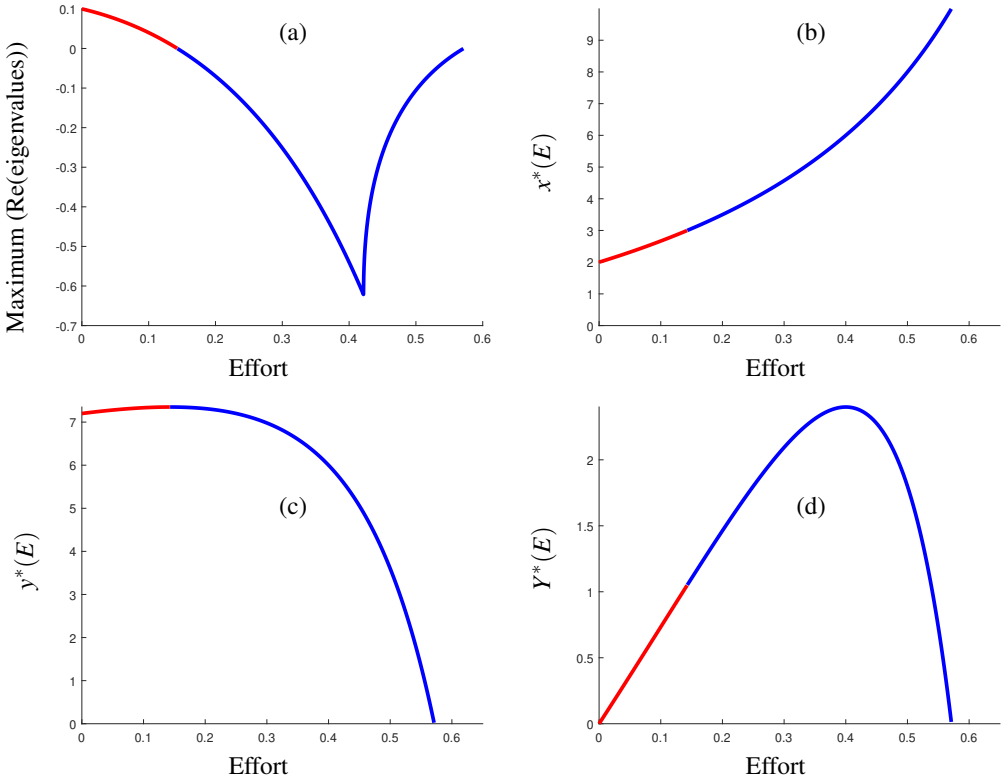

FIGURE 1. (a) Evaluation of the maximum real part of the eigenvalues relative to the effort employed on the predator. (b) and (c) The variation of the total prey and the total predator density, respectively. (d) The yield curve shows a maximum at stable state. The figures are generated for the specified parameters $r = 3, K = 10, a = 2, e = 0.75, D = 4, d = 0.5$. The blue (resp. red) color indicates the effort value for which the equilibrium is stable (resp. unstable).

where $\Gamma := (\gamma_{ij})$ and $\Theta := (\theta_{ij})$ are the matrices representing the migration terms of prey and predator between the n patches with

$$\gamma_{ii} := -\sum_{j=1, j\neq i}^{n} \gamma_{ji}, \qquad \theta_{ii} := -\sum_{j=1, j\neq i}^{n} \theta_{ji}. \tag{3.2}$$

Recall that, if Γ (respectively Θ) is irreducible, then the kernel of the matrix Γ (respectively Θ) is generated by a positive vector, (see A). In all of this paper, we denote by $\delta := (\delta_1, \ldots, \delta_n)^T$ resp. $\xi := (\xi_1, \ldots, \xi_n)^T$ this positive vector. For more details on the proprieties of the matrices Γ resp. Θ, see A. Figure 2 shows the system of n connected patches. The fish prey and predator can move in n patches.

The model (3.1) has been considered by Auger *et al.* [8] for particular case of two patches connected by migrations and the same predation in each patch, *i.e.* $a_1 = a_2$ and $d_1 = d_2$.

Considering the population movement between patches, predator and prey dynamics in patch i are governed by the following equations:

$$\begin{cases} \dfrac{\mathrm{d}x_i}{\mathrm{d}t} = f_i(x_i, y_i) + \epsilon \displaystyle\sum_{j=1}^{n} \gamma_{ij} x_j, \\ \dfrac{\mathrm{d}y_i}{\mathrm{d}t} = g_i(x_i, y_i) + \epsilon \displaystyle\sum_{j=1}^{n} \theta_{ij} y_j, \end{cases} \qquad i = 1, \cdots, n, \tag{3.3}$$

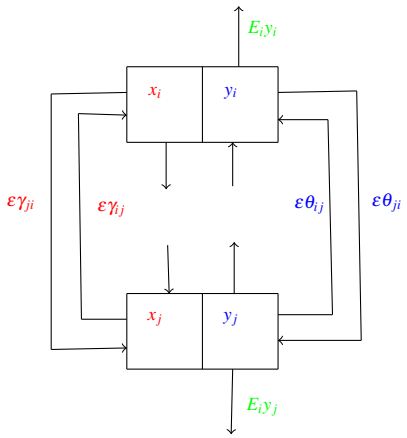

FIGURE 2. A coupled predator–prey system with harvesting of predators in n patches.

The functions f_i and g_i account for the predator–prey interactions and the harvesting. Thus, the compact form of the model (3.1) is

$$\dot{\mathbf{Z}} = \mathbf{H}(\mathbf{Z}) + \epsilon \mathscr{D}\mathbf{Z},$$

where $\mathbf{H}(\mathbf{Z}) = (\mathbf{F}(\mathbf{Z}), \mathbf{G}(\mathbf{Z}))^T$ with $\mathbf{F}(\mathbf{Z}) = (f_1(x_1, y_1), \ldots, f_n(x_n, y_n))^T$ and $\mathbf{G}(\mathbf{Z}) = (g_1(x_1, y_1), \ldots, g_n(x_n, y_n))^T$. The matrix $\mathscr{D}$ is the movement matrix for both the populations so that its block diagonal form can be written as

$$\mathscr{D} = \begin{pmatrix} \Gamma & 0 \\ 0 & \Theta \end{pmatrix}.$$

We refer the reader to [42, 43] for detailed interpretations of predator–prey models and parameters. As to the non-negativity of the solution, we have the following proposition:

Proposition 3.1. *The domain* $\mathbb{R}^{2n}_+ = \{(x_1, \ldots, x_n; y_1, \ldots, y_n) \in \mathbb{R}^{2n} : x_i \geq 0 \text{ and } y_i \geq 0, i = 1, \ldots, n\}$ *is positively invariant for the system* (3.1).

Proof. Assume that $x_j, y_j \geq 0$ for all j and there exists i such that $x_i = 0$ resp. $y_i = 0$. We have $\frac{\mathrm{d}x_i}{\mathrm{d}t}(x_i = 0) = \epsilon \sum_{j \neq i} \gamma_{ij} x_j \geq 0$ resp. $\frac{\mathrm{d}y_i}{\mathrm{d}t}(y_i = 0) = \epsilon \sum_{j \neq i} \theta_{ij} x_j \geq 0$. Hence, on the boundary of $\mathbb{R}^{2n}_+$, the vector field associated to (3.1) either is tangent to the boundary of $\mathbb{R}^{2n}_+$, or points inward. According to [44], Proposition B.7, page 267, no trajectory comes out of $\mathbb{R}^{2n}_+$. Therefore, $\mathbb{R}^{2n}_+$ is positively invariant for (3.1). □

In all this work, if the system (3.1) has a unique equilibrium in the interior of the positive cone $\mathbb{R}^{2n}_+$, we denote this equilibrium by $\mathbb{E}^*_{2n}(\epsilon, E_1, \ldots, E_n)$ and its components by

$$(x_1^*(\epsilon, E_1, \ldots, E_n), \ldots, x_n^*(\epsilon, E_1, \ldots, E_n); y_1^*(\epsilon, E_1, \ldots, E_n), \ldots, y_n^*(\epsilon, E_1, \ldots, E_n)).$$

i.e., in the case where $\epsilon = 0$, the dynamics of each patch in system (3.1) are governed by

$$\begin{cases} \dfrac{\mathrm{d}x_i}{\mathrm{d}t} = r_i x_i \left(1 - \dfrac{x_i}{K_i}\right) - \dfrac{a_i x_i y_i}{x_i + D}, \\ \dfrac{\mathrm{d}y_i}{\mathrm{d}t} = \left(e \dfrac{a_i x_i}{x_i + D} - d_i\right) y_i - E_i y_i. \end{cases} \quad i = 1, \cdots, n, \tag{3.4}$$

Assuming that $d_i + E_i < ea_i \frac{K_i}{K_i+D_i}$ for all i, the last system admits the following non-trivial equilibrium point in the positive cone $\mathbb{R}^{2n}_+$:

$$(x_1^*(0,E_1),\dots,x_n^*(0,E_n),y_1^*(0,E_1),\dots,y_n^*(0,E_n)),$$

where

$$x_i^*(0,E_i) = \frac{(d_i+E_i)D_i}{ea_i - d_i - E_i}, \quad \text{for all } i = 1,\dots,n,$$

and

$$y_i^*(0,E_i) = \frac{r_i D_i}{a_i}\left(1 + \frac{d_i+E_i}{ea_i-d_i-E_i}\right)\left(1 - \frac{D_i(d_i+E_i)}{K_i(ea_i-d_i-E_i)}\right).$$

4. Two time scale dynamics

In the upcoming sections, our focus is on examining the behavior of model (3.1) as the migration rate ϵ tends to infinity. This analysis is conducted using singular perturbation theory and Tikhonov's theorem [34, 35]. To avoid any confusion with $(X(t),Y(t))$, which represents the total population, we denote by $(U(t),V(t))$ the solution of the predator- prey model with harvesting (4.1). We establish that, as ϵ approaches infinity, $(X(t),Y(t))$ becomes asymptotically equivalent to $(U(t),V(t))$. The following result is then obtained:

Theorem 4.1. *Let $(x_1(t,\epsilon),\dots,x_n(t,\epsilon);y_1(t,\epsilon),\dots,y_n(t,\epsilon))$ be the solution of the system (3.1) with initial condition $(x_1^0,\cdots,x_n^0;y_1^0,\cdots,y_n^0)$ satisfying $x_i^0,y_i^0 \geq 0$ for $i = 1\cdots n$. Let $(U(t),V(t))$ be the solution of the following system:*

$$\begin{cases} \dfrac{dX}{\mathrm{d}t} = rX\left(1-\dfrac{X}{K}\right) - \varphi(X)Y, \\ \dfrac{dY}{\mathrm{d}t} = (e\varphi(X) - \mathrm{d})\,Y - EY, \end{cases} \tag{4.1}$$

where

$$r = \frac{\sum_{i=1}^n \delta_i r_i}{\sum_{i=1}^n \delta_i}, \quad K = \sum_{i=1}^n \delta_i \frac{\sum_{i=1}^n \delta_i r_i}{\sum_{i=1}^n \delta_i^2 \alpha_i}, \quad \varphi(X) = \frac{X}{\sum_{i=1}^n \xi_i}\sum_{i=1}^n \frac{a_i\delta_i\xi_i}{\delta_i X + (\sum_{i=1}^n \delta_i)\,D_i}, \tag{4.2}$$
$$d = \frac{\sum_{i=1}^n \xi_i d_i}{\sum_{i=1}^n \xi_i} \quad \text{and} \quad E = \frac{\sum_{i=1}^n \xi_i E_i}{\sum_{i=1}^n \xi_i} \quad \text{with } \alpha_i = \frac{r_i}{K_i}, \quad \ker\Gamma = <\delta>, \quad \ker\Theta = <\xi>,$$

with initial condition $(X_0,Y_0) = \left(\sum_{i=1}^n x_i^0, \sum_{i=1}^n y_i^0\right)$. *Then, when $\epsilon \to \infty$, we have*

$$\begin{cases} \sum_{i=1}^n x_i(t,\epsilon) = U(t) + o_\epsilon(1), \\ \sum_{i=1}^n y_i(t,\epsilon) = V(t) + o_\epsilon(1) \end{cases} \quad \text{uniformly for } t \in [0,T] \tag{4.3}$$

and, for any $t_0 > 0$, we have

$$\begin{cases} x_i(t,\epsilon) = \dfrac{\delta_i}{\sum_{i=1}^n \delta_i} U(t) + o_\epsilon(1), \\ y_i(t,\epsilon) = \dfrac{\xi_i}{\sum_{i=1}^n \xi_i} V(t) + o_\epsilon(1), \end{cases} \quad i = 1,\dots,n, \ \textit{uniformly for} \quad t \in [t_0, T], \tag{4.4}$$

where $0 < t_0 < T$ are arbitrary but fixed and independent of ϵ. If the solution $(U(t), V(t))$ of the reduced problem converges to an asymptotically stable equilibrium, then we can put $T = +\infty$ in Approximations (4.3) and (4.4).

Proof. Let $X(t,\epsilon) = \sum_{i=1}^n x_i(t,\epsilon)$ and $Y(t,\epsilon) = \sum_{i=1}^n y_i(t,\epsilon)$. We rewrite the system (3.3) using the variables $(X, x_1, \cdots, x_{n-1}; Y, y_1, \cdots, y_{n-1})$, and get:

$$\begin{cases} \dfrac{dX}{\mathrm{d}t} &= \displaystyle\sum_{i=1}^n \left\{ r_i x_i \left(1 - \frac{x_i}{K_i}\right) - \frac{a_i x_i y_i}{x_i + D_i} \right\}, \\ \dfrac{\mathrm{d}x_i}{\mathrm{d}t} &= r_i x_i \left(1 - \dfrac{x_i}{K_i}\right) - \dfrac{a_i x_i y_i}{x_i + D_i} + \epsilon \displaystyle\sum_{j=1, j\neq i}^n (\gamma_{ij} x_j - \gamma_{ji} x_i), \quad i = 1, \cdots, n-1, \\ \dfrac{dY}{\mathrm{d}t} &= \displaystyle\sum_{i=1}^n \left\{ \left(e\frac{a_i x_i}{x_i + D_i} - d_i \right) y_i - E_i y_i \right\}, \\ \dfrac{\mathrm{d}y_i}{\mathrm{d}t} &= \left(e\dfrac{a_i x_i}{x_i + D_i} - d_i \right) y_i - E_i y_i + \epsilon \displaystyle\sum_{j=1, j\neq i}^n (\theta_{ij} y_j - \theta_{ji} y_i), \quad i = 1, \cdots, n-1. \end{cases} \tag{4.5}$$

This system is actually a system in the variables $(X, x_1, \cdots, x_{n-1}; Y, y_1, \cdots, y_{n-1})$, since, whenever x_n and y_n appears in the right hand side of (4.5), it should be replaced by

$$x_n = X - \sum_{i=1}^{n-1} x_i, \text{ and } y_n = Y - \sum_{i=1}^{n-1} y_i. \tag{4.6}$$

When $\epsilon \to \infty$, (4.5) is a *slow–fast* system, with two *slow variables*, X, Y, and $2n-2$ *fast variables*, x_i, y_i for $i = 1 \cdots n-1$. As suggested by Tikhonov's theorem [34, 35], we consider the dynamics of the fast variables in the time scale $\tau = \epsilon t$. We get

$$\begin{cases} \dfrac{\mathrm{d}x_i}{\mathrm{d}\tau} = \dfrac{1}{\epsilon} r_i x_i \left(1 - \dfrac{x_i}{K_i}\right) - \dfrac{1}{\epsilon} \dfrac{a_i x_i y_i}{x_i + D_i} + \displaystyle\sum_{j=1, j\neq i}^n (\gamma_{ij} x_j - \gamma_{ji} x_i), \\ \dfrac{\mathrm{d}y_i}{\mathrm{d}\tau} = \dfrac{1}{\epsilon} \left(e\dfrac{a_i x_i}{x_i + D_i} - d_i \right) y_i - \dfrac{1}{\epsilon} E_i y_i + \displaystyle\sum_{j=1, j\neq i}^n (\theta_{ij} y_j - \theta_{ji} y_i) \end{cases} \quad i = 1, \cdots, n-1.$$

where x_n and y_n are given by (4.6). For time scale separation methods we also refer to methods of aggregation of variables based on the center manifold theorem, [45] and [46]. In the limit $\epsilon \to \infty$, we find the *fast dynamics*

$$\begin{cases} \dfrac{\mathrm{d}x_i}{\mathrm{d}\tau} = \displaystyle\sum_{j=1, j\neq i}^n (\gamma_{ij} x_j - \gamma_{ji} x_i), \\ \dfrac{\mathrm{d}y_i}{\mathrm{d}\tau} = \displaystyle\sum_{j=1, j\neq i}^n (\theta_{ij} y_j - \theta_{ji} y_i) \end{cases} \quad i = 1, \cdots, n-1.$$

This is an $2n-2$ dimensional linear system differential in the variable $(Z_1, Z_2) := (x_1, \cdots, x_{n-1}; y_1, \cdots, y_{n-1})$, which can be rewritten in matricial form:

$$\begin{cases} \dot{Z}_1 = \mathscr{L}_1 Z_1 + XV_1, \\ \dot{Z}_2 = \mathscr{L}_2 Z_2 + YV_2, \end{cases} \tag{4.7}$$

with $\mathscr{L}_k := L_k - U_k, k = 1, 2$ where $L_1 := (\gamma_{ij})_{n-1\times n-1}$ (resp. $L_2 := (\theta_{ij})_{n-1\times n-1}$) is the submatrix of the matrix Γ (resp. Θ), obtained by dropping the last row and the last column of Γ (resp. Θ), V_1 (resp. V_2) is the vector defined by $V_1 := (\gamma_{in})_{n-1\times 1}$ (resp. $V_2 := (\theta_{in})_{n-1\times 1}$) and $U_k = (V_k; \ldots; V_k)$ for $k = 1, 2$. By Lemma A.1, the matrices $\mathscr{L}_1$ and $\mathscr{L}_2$ are stable, meaning all their eigenvalues have negative real parts. Therefore, they are invertible, and the equilibrium of the system (4.7) is globally asymptotically stable (GAS). This equilibrium is given by:

$$\left(\frac{\delta_1}{\sum_{i=1}^n \delta_i} X, \ldots, \frac{\delta_{n-1}}{\sum_{i=1}^n \delta_i} X; \frac{\xi_1}{\sum_{i=1}^n \xi_i} Y, \ldots, \frac{\xi_{n-1}}{\sum_{i=1}^n \xi_i} Y\right)^T.$$

Indeed, we denote by $L_k^{(i)}, U_k^{(i)}$ and $V_k^{(i)}$ the ith row of the matrix L_k, U_k and the vector V_k respectively. We have:

$$\begin{aligned} \frac{\delta_n}{\sum_{i=1}^n \delta_i}\left(L_1^{(i)} - U_1^{(i)}\right)\begin{pmatrix} \frac{\delta_1}{\delta_n} X & \ldots & \frac{\delta_{n-1}}{\delta_n} X \end{pmatrix}^T &= -\frac{\delta_n}{\sum_{i=1}^n \delta_i} X\gamma_{in} - \frac{\sum_{i=1}^{n-1} \delta_i}{\sum_{i=1}^n \delta_i} X\gamma_{in} \\ &= -X\gamma_{in} = -XV_1^{(i)}, \end{aligned}$$

and

$$\begin{aligned} \frac{\xi_n}{\sum_{i=1}^n \xi_i}\left(L_2^{(i)} - U_2^{(i)}\right)\begin{pmatrix} \frac{\xi_1}{\xi_n} Y & \ldots & \frac{\xi_{n-1}}{\xi_n} Y \end{pmatrix}^T &= -\frac{\xi_n}{\sum_{i=1}^n \xi_i} Y\theta_{in} - \frac{\sum_{i=1}^{n-1} \xi_i}{\sum_{i=1}^n \xi_i} Y\theta_{in} \\ &= -Y\theta_{in} = -YV_2^{(i)}, \end{aligned}$$

Thus, the slow manifold of system (4.5), which corresponds to the equilibrium point of the fast dynamics, is unique and given by:

$$\begin{cases} x_i = \dfrac{\delta_i}{\sum_{i=1}^n \delta_i} X, \\ y_i = \dfrac{\xi_i}{\sum_{i=1}^n \xi_i} Y, \end{cases} \qquad i = 1, \ldots, n-1. \tag{4.8}$$

As this manifold is GAS, Tikhonov's theorem ensures that, after a fast transition toward the slow manifold, the solutions of (4.5) are approximated by the solutions of the *reduced model*, which is obtained by replacing (4.8) into the dynamics of the slow variable, that is:

$$\begin{cases} \dfrac{dX}{\mathrm{d}t} = \displaystyle\sum_{i=1}^n \left\{ r_i \frac{\delta_i}{\sum_{i=1}^n \delta_i} X\left(1 - \frac{\delta_i}{\left(\sum_{i=1}^n \delta_i\right) K_i} X\right) - \frac{a_i \dfrac{\delta_i}{\sum_{i=1}^n \delta_i} \dfrac{\xi_i}{\sum_{i=1}^n \xi_i} XY}{\dfrac{\delta_i}{\sum_{i=1}^n \delta_i} X + D_i} \right\}, \\ \dfrac{dY}{\mathrm{d}t} = \displaystyle\sum_{i=1}^n \left\{ \left(e \frac{a_i \dfrac{\delta_i}{\sum_{i=1}^n \delta_i} X}{\dfrac{\delta_i}{\sum_{i=1}^n \delta_i} X + D_i} - d_i \right) \frac{\xi_i}{\sum_{i=1}^n \xi_i} Y - \frac{\xi_i E_i}{\sum_{i=1}^n \xi_i} Y; \right\}. \end{cases}$$

Therefore, we obtain the reduced model (4.1) where r, K, φ, d and E are defined in (4.2). □

We denote by H the following assumption:

H. The matrix of migration Γ is symmetric and the predation parameters D_i in each patch are equal, denote D this common value.

In general, its difficult to calculate explicitly the equilibrium of the coexistence of the reduced model (4.1), except in special particular case as shown in the following Corollary:

Corollary 4.2. *Assume that H is satisfied. Let $(x_1(t,\epsilon),\dots,y_n(t,\epsilon);y_1(t,\epsilon),\dots,y_n(t,\epsilon))$ be the solution of the system (3.1). Let $(U(t),V(t))$ be the solution of the following predator- prey model*

$$\begin{cases} \dfrac{dX}{\mathrm{d}t} = rX\left(1-\dfrac{X}{K}\right) - a\dfrac{XY}{X+nD}, \\ \dfrac{dY}{\mathrm{d}t} = \left(ea\dfrac{X}{X+nD} - \mathrm{d}\right)Y - EY, \end{cases} \tag{4.9}$$

where

$$r = \frac{\sum_{i=1}^n r_i}{n}, \quad K = n\frac{\sum_{i=1}^n r_i}{\sum_{i=1}^n \alpha_i}, \quad d = \frac{\sum_{i=1}^n \xi_i d_i}{\sum_{i=1}^n \xi_i} \quad E = \frac{\sum_{i=1}^n \xi_i E_i}{\sum_{i=1}^n \xi_i} \text{ and } \quad a = \frac{\sum_{i=1}^n \xi_i a_i}{\sum_{i=1}^n \xi_i} \tag{4.10}$$

with initial condition $(X_0,Y_0) = \left(\sum_{i=1}^n x_i^0, \sum_{i=1}^n y_i^0\right)$. Then, when $\epsilon \to \infty$, we have

$$\begin{cases} \sum_{i=1}^n x_i(t,\epsilon) = U(t) + o_\epsilon(1), \\ \sum_{i=1}^n y_i(t,\epsilon) = V(t) + o_\epsilon(1) \end{cases} \qquad \text{uniformly for } t \in [0,T] \tag{4.11}$$

and, for any $t_0 > 0$, we have

$$\begin{cases} x_i(t,\epsilon) = \dfrac{U(t)}{n} + o_\epsilon(1), \\ y_i(t,\epsilon) = \dfrac{\xi_i}{\sum_{i=1}^n \xi_i} V(t) + o_\epsilon(1), \end{cases} \qquad i = 1,\dots,n, \text{ uniformly for } \quad t \in [t_0,T], \tag{4.12}$$

where $0 < t_0 < T$ are arbitrary but fixed and independent of ϵ.

Proof. If the matrix of migration Γ is symmetric then $\delta_i = 1$ for all i. By subsituting in (4.1) and (4.2) we obtain (4.9) and (4.10). □

Corollary 4.3. *Assume that H is satisfied.If $d + E < ea\frac{K}{K+nD}$, then the reduced model (4.9) admits (X^*,Y^*) with*

$$(X^*(E),Y^*(E)) = \left(\frac{nD(d+E)}{ea-d-E}, \frac{rnD}{a}\left(1+\frac{d+E}{ea-d-E}\right)\left(1-\frac{nD(d+E)}{K(ea-d-E)}\right)\right),$$

as positive equilibrium. Moreover,

- *If $ea\frac{K-nD}{K+nD} \le d+E \le ea\frac{K}{K+nD}$, then $(X^*(E),Y^*(E))$ is globally asymptotically stable in the positive quadrant.*

- *If $d+E \leq ea\frac{K-nD}{K+nD}$, then $(X^*(E), Y^*(E))$ is unstable and each orbit in the positive quadrant except the positive equilibrium converges to a periodic orbit. It is also known that the periodic orbit is unique.*
- *If $ea\frac{K}{K+nD} < d+E$, the predator goes extinct, the positive equilibrium does not exist in the nonnegative quadrant and $(K,0)$ is globally asymptotically stable.*

Proof. Direct calculation gives the equilibrium $(X^*(E), Y^*(E))$ and by [41, 47] we conclude the stability conditions. □

As consequence direct of the previous corollary, if $ea\frac{K-nD}{K+nD} < d+E < ea\frac{K}{K+nD}$, when t and ϵ tend to infinity, the density population $x_i(t,\epsilon)$ and $y_i(t,\epsilon)$ for all i tends toward respectively

$$x_i^*(\infty, E) = \frac{D(d+E)}{ea-d-E} \tag{4.13}$$

and

$$y_i^*(\infty, E) = \frac{\xi_i}{\sum_{i=1}^n \xi_i}\frac{rD}{a}\left(1+\frac{d+E}{ea-d-E}\right)\left(1-\frac{nD(d+E)}{K(ea-d-E)}\right). \tag{4.14}$$

5. Total yields at MSY

In this part, we consider the predator- prey model with n patches connected by migration terms as described in (3.1). Assume that the system (3.1) has a positive equilibrium, denoted by

$$\mathbb{E}_{2n}^* = (x_1^*(\epsilon, E_1, \ldots, E_n), \ldots, x_n^*(\epsilon, E_1, \ldots, E_n); y_1^*(\epsilon, E_1, \ldots, E_n), \ldots, y_n^*(\epsilon, E_1, \ldots, E_n))$$

which depends on the migration rate ϵ and the fishing efforts across all patches. First, we present the following result:

Proposition 5.1. *For all $\epsilon \geq 0$, the total Maximum Sustainable Yield (MSY), given as the sum of the MSY from each patch i is expressed as:*

$$Y_{MSY,T}^*(\epsilon) = \max_{(E_1,\ldots,E_n)} \sum_{i=1}^n \left\{ \frac{r_i}{a_i}(x_i^*+D_i)E_i\left(1-\frac{x_i^*}{K_i}\right) + \frac{(x_i^*+D_i)E_i}{a_i x_i^*}\epsilon\sum_{j=1}^n \gamma_{ij}x_j^* \right\}. \tag{5.1}$$

In particular, for $\epsilon = 0$, we have

$$Y_{MSY,T}^*(0) = \sum_{i=1}^n \frac{r_i}{4a_iK_i}\frac{(K_i(ea_i-d_i)-d_iD_i)^2}{ea_i-d_i}. \tag{5.2}$$

Proof. The components $x_i^*(\epsilon; E_1, \ldots, E_n)$ and $y_i^*(\epsilon; E_1, \ldots, E_n)$ for $i = 1, \ldots, n$ of the equilibrium $\mathbb{E}_{2n}^*$ satisfy the following equations:

$$r_i x_i^*(\epsilon; E_1, \ldots, E_n)\left(1-\frac{x_i^*(\epsilon; E_1, \ldots, E_n)}{K_i}\right) - \frac{a_i x_i^*(\epsilon; E_1, \ldots, E_n) y_i^*(\epsilon; E_1, \ldots, E_n)}{x_i^*(\epsilon; E_1, \ldots, E_n)+D_i}$$
$$+\epsilon\sum_{j=1}^n \gamma_{ij}x_j^*(\epsilon; E_1, \ldots, E_n) = 0 \quad i = 1, \ldots, n.$$

For all $i = 1, \dots, n$, the yield Y_i^* of patch i is given by

$$Y_i^*(\epsilon; E_1, \dots, E_n) = E_i y_i^*(\epsilon; E_1, \dots, E_n) = \frac{r_i}{a_i}(x_i^*(\epsilon; E_1, \dots, E_n) + D_i)E_i \left(1 - \frac{x_i^*(\epsilon; E_1, \dots, E_n)}{K_i}\right)$$
$$+ \frac{(x_i^*(\epsilon; E_1, \dots, E_n) + D_i)E_i}{a_i x_i^*(\epsilon; E_1, \dots, E_n)} \epsilon \sum_{j=1}^{n} \gamma_{ij} x_j^*(\epsilon; E_1, \dots, E_n).$$

The sum of Y_i^* for $i = 1, \dots, n$ gives the total Yield Y_T^* of n connected patches:

$$Y_T^*(\epsilon; E_1, \dots, E_n) = \sum_{i=1}^{n} \left\{ \frac{r_i}{a_i}(x_i^* + D_i)E_i \left(1 - \frac{x_i^*}{K_i}\right) + \frac{(x_i^* + D_i)E_i}{a_i x_i^*} \epsilon \sum_{j=1}^{n} \gamma_{ij} x_j^* \right\}. \tag{5.3}$$

Hence, the maximum of the previous formula (5.3) gives the total MSY (5.1).
For $\epsilon = 0$, the sum of MSY of each isolated patch take the following form:

$$\begin{aligned}
Y_{MSY,T}^*(0) &= \max_{(E_1,\dots,E_n)} \sum_{i=1}^{n} \left\{ \frac{r_i}{a_i}(x_i^*(0; E_i) + D_i)E_i \left(1 - \frac{x_i^*(0; E_i)}{K_i}\right) \right\}. \\
&= \max_{(E_1,\dots,E_n)} \sum_{i=1}^{n} \left\{ \frac{r_i}{a_i} \left(\frac{(d_i + E_i)D_i}{ea_i - d_i - E_i} + D_i \right) E_i \left(1 - \frac{\frac{(d_i+E_i)D_i}{ea_i - d_i - E_i}}{K_i}\right) \right\}. \\
&= \sum_{i=1}^{n} \max_{E_i} \left\{ \frac{r_i D_i E_i}{a_i} \left(1 + \frac{d_i + E_i}{ea_i - d_i - E_i}\right) \left(1 - \frac{D_i(d_i + E_i)}{K_i(ea_i - d_i - E_i)}\right) \right\} \\
&= \sum_{i=1}^{n} \frac{r_i}{4a_i K_i} \frac{(K_i(ea_i - d_i) - d_i D_i)^2}{ea_i - d_i},
\end{aligned}$$

since $x_i^*(0, E_i) = \frac{(d_i+E_i)D_i}{ea_i - d_i - E_i}$ for all $i = 1, \dots, n$. This completes the proof of Proposition. □

Under the assumption H, for $\epsilon = 0$, the sum of MSY of each isolated patch take the following form:

$$Y_{MSY,T}^*(0) = \sum_{i=1}^{n} \frac{r_i}{4a_i K_i} \frac{(K_i(ea_i - d_i) - d_i D)^2}{ea_i - d_i}, \tag{5.4}$$

and, when the migration is large, we obtain the following corollary:

Corollary 5.2. *When $\epsilon \to \infty$, we have:*

$$E_{MSY,\infty}^* = \frac{(ea - d)[K(ea - d) - ndD]}{K(ea - d) - ndD + 2eanD},$$

and the corresponding Maximum Sustainable Yield (MSY) is:

$$Y_{MSY,T}^*(\infty) = \frac{r}{4aK} \frac{(K(ea - d) - ndD)^2}{ea - d}. \tag{5.5}$$

Proof. When $\epsilon \to \infty$, the dynamics reduce to the simplified model (4.9). From this reduced model, the expression for $Y_T^*(\infty; E)$ is:

$$Y_T^*(\infty; E) = EY^*(E) = \frac{rDn}{a} E \left(1 + \frac{d+E}{ea-d-E}\right)\left(1 - \frac{nD(d+E)}{K(ea-d-E)}\right).$$

Here, the parameters r, K, a, d, n and D are defined in (4.10), and D is the common value of the predation parameters D_i assumed equal in each patch under hypothesis H. Therefore, we conclude that:

$$E^*_{MSY,\infty} = \frac{(ea-d)[K(ea-d) - ndD]}{K(ea-d) - ndD + 2eanD},$$

which represents the equilibrium fishing effort that maximizes sustainable yield under the assumption $\epsilon \to \infty$.

Substituting $E^*_{MSY,\infty}$ back into the expression for $Y_T^*(\infty; E)$, the MSY is given by:

$$Y^*_{MSY,T}(\infty) = \frac{r}{4aK} \frac{(K(ea-d) - ndD)^2}{ea-d}.$$

□

Now, we will compare the yield at MSY for the reduced system (4.9), denoted by $Y^*_{MSY,T}(\infty)$ as given in (5.5) with the sum of yields for n isolated patches, denoted by $Y^*_{MSY,T}(0)$, as presented in (5.4). We define the yield excess, $\Delta Y^*_{MSY,T}$ as follows:

$$\Delta Y^*_{MSY,T} = Y^*_{MSY,T}(\infty) - Y^*_{MSY,T}(0). \tag{5.6}$$

We deduce that:

$$\Delta Y^*_{MSY,T} > 0 \iff \frac{r}{4aK} \frac{(K(ea-d) - ndD)^2}{ea-d} > \sum_{i=1}^{n} \frac{r_i}{4a_iK_i} \frac{(K_i(ea_i - d_i) - d_iD)^2}{ea_i - d_i}. \tag{5.7}$$

5.1. Homogeneous case

Let us consider the model (3.1) where the patches have a homogeneous structure, meaning that the parameters r_i, K_i, a_i and d_i are independent of the patch. We also assume that the movement of prey between patches is symmetric. In the next proposition, we will show that if the n patches are identical, then at MSY, the yield for the reduced system (4.9), denoted by $Y^*_{MSY,T}(\infty)$, as given in (5.5) is equal to the sum of the yields from n isolated patches, denoted by $Y^*_{MSY,T}(0)$ in (5.4). Mathematically, we can express the following result:

Proposition 5.3. *Assume that H is satisfied, $r_1 = \ldots = r_n =: r_0, K_1 = \ldots = K_n =: K_0, a_1 = \ldots = a_n =: a_0$ and $d_1 = \ldots = d_n =: d_0$. Then,*

$$Y^*_{MSY,T}(\infty) = Y^*_{MSY,T}(0) = \frac{nr_0}{4a_0K_0} \frac{(K_0(ea_0 - d_0) - d_0D)^2}{ea_0 - d_0}.$$

Proof. Under the assumptions of the previous proposition, the parameters of the reduced model (4.9) becomes as:

$$r = r_0, \quad K = nK_0, \quad a = a_0, \quad \text{and} \quad d = d_0.$$

After substitution in $Y^*_{MSY,T}(\infty)$ and $Y^*_{MSY,T}(0)$, it comes:

$$Y^*_{MSY,T}(\infty) = \frac{nr_0}{4a_0K_0}\frac{(K_0(ea_0-d_0)-d_0D)^2}{ea_0-d_0}, \tag{5.8}$$

and,

$$Y^*_{MSY,T}(0) = \sum_{i=1}^{n}\frac{r_0}{4a_0K_0}\frac{(K_0(ea_0-d_0)-d_0D)^2}{ea_0-d_0} = \frac{nr_0}{4a_0K_0}\frac{(K_0(ea_0-d_0)-d_0D)^2}{ea_0-d_0}. \tag{5.9}$$

Subtracting (5.8) and (5.9) we get the equality between $Y^*_{MSY,T}(\infty)$ and $Y^*_{MSY,T}(0)$. □

This proposition shows that, under the specified conditions of homogeneous patches and symmetric prey movement between patches, the total yield at MSY for the interconnected system of patches is equal to the sum of yields at MSY for each isolated patch. This result underscores the fact that homogeneity and symmetry of prey in the system allow for a straightforward summation of individual patch yields to determine the overall system yield at MSY.

5.2. Heterogeneous case

Let us now consider a heterogeneous scenario where the parameters r_i, K_i, a_i, and d_i depend on the patch i. In this part, we aim to prove that, at the Maximum Sustainable Yield (MSY), the yield for the reduced system (4.9), denoted as $Y^*_{MSY,T}(\infty)$, can be greater than, equal to, or smaller than the sum of the MSY yields for n isolated patches, *i.e.*, $Y^*_{MSY,T}(0)$.

Let us define the following terms:

- $\Upsilon(D)$: The total MSY for the reduced system, $Y^*_{MSY,T}(\infty)$.
- $\Upsilon_i(D)$ for $i = 1, \dots, n$: The MSY for patch i in the case where inter-patch interactions are absent, *i.e.*, $\epsilon = 0$.

We now introduce the function Φ as follows:

$$\begin{aligned}
\Phi(D) &:= \Upsilon(D) - \sum_{i=1}^{n}\Upsilon_i(D)\\
&= \frac{r}{4aK}\frac{(K(ea-d)-ndD)^2}{ea-d} - \sum_{i=1}^{n}\frac{r_i}{4a_iK_i}\frac{(K_i(ea_i-d_i)-d_iD)^2}{ea_i-d_i}\\
&= \frac{r}{4aK(ea-d)}\left[K^2(ea-d)^2+(ndD)^2-2K(ea-d)ndD\right]\\
&\quad - \sum_{i=1}^{n}\left\{\frac{r_i}{4a_iK_i(ea_i-d_i)}\left[K_i^2(ea_i-d_i)^2+(nd_iD)^2-2K_i(ea_i-d_i)nd_iD\right]\right\}\\
&= \frac{rK(ea-d)}{4a} + \frac{rn^2d^2}{4aK(ea-d)}D^2 - \frac{rnd}{2a}D\\
&\quad - \sum_{i=1}^{n}\frac{r_iK_i(ea_i-d_i)}{4a_i} - \left(\sum_{i=1}^{n}\frac{r_in^2d_i^2}{4a_iK_i(ea_i-d_i)}\right)D^2 + \left(\sum_{i=1}^{n}\frac{r_ind_i}{2a_i}\right)D,\\
&= \left(\frac{rK(ea-d)}{4a} - \sum_{i=1}^{n}\frac{r_iK_i(ea_i-d_i)}{4a_i}\right) + \left(-\frac{rnd}{2a} + \sum_{i=1}^{n}\frac{r_ind_i}{2a_i}\right)D\\
&\quad + \left(\frac{rn^2d^2}{4aK(ea-d)} - \sum_{i=1}^{n}\frac{r_in^2d_i^2}{4a_iK_i(ea_i-d_i)}\right)D^2.
\end{aligned} \tag{5.10}$$

Therefore, $\Phi(D) = \kappa_0 + \kappa_1 D + \kappa_2 D^2$ where

$$\begin{cases} \kappa_0 = \dfrac{rK(ea-d)}{4a} - \sum_{i=1}^{n} \dfrac{r_i K_i (ea_i - d_i)}{4a_i}, \\ \kappa_1 = -\dfrac{rnd}{2a} + \sum_{i=1}^{n} \dfrac{r_i n d_i}{2a_i}, \\ \kappa_2 = \dfrac{rn^2 d^2}{4aK(ea-d)} - \sum_{i=1}^{n} \dfrac{r_i n^2 d_i^2}{4a_i K_i (ea_i - d_i)}. \end{cases}$$

Note that, Φ is the Yield excess which can written as follows:

$$\Phi(D) := \Delta Y^*_{MSY}(D) = Y^*_{MSY,T}(\infty) - Y^*_{MSY,T}(0). \tag{5.11}$$

Our aim is to study the sign of the function Φ as a function of the parameter D. First, we present the following result:

Theorem 5.4. *Assume that $\kappa_2 = 0$. We distinguish the following situations:*

1. If** $\kappa_0 > 0$**:

$$\begin{aligned} &\textit{(i) If } \kappa_1 \geq 0, \quad \Delta Y^*_{MSY}(D) > 0 \quad \textit{for all } D > 0, \\ &\textit{(ii) If } \kappa_1 < 0, \quad \begin{cases} \Delta Y^*_{MSY}(D) < 0, & \textit{if } D > -\dfrac{\kappa_0}{2\kappa_1}, \\ \Delta Y^*_{MSY}(D) = 0, & \textit{if } D = -\dfrac{\kappa_0}{2\kappa_1}, \\ \Delta Y^*_{MSY}(D) > 0, & \textit{if } D < -\dfrac{\kappa_0}{2\kappa_1}. \end{cases} \end{aligned}$$

2. If** $\kappa_0 = 0$**:

$$\begin{aligned} &\textit{(i) If } \kappa_1 > 0, \quad \Delta Y^*_{MSY}(D) > 0 \quad \textit{for all } D > 0, \\ &\textit{(ii) If } \kappa_1 = 0, \quad \Delta Y^*_{MSY}(D) = 0 \quad \textit{for all } D > 0, \\ &\textit{(iii) If } \kappa_1 < 0, \quad \Delta Y^*_{MSY}(D) < 0 \quad \textit{for all } D > 0. \end{aligned}$$

3. If** $\kappa_0 < 0$**:

$$\begin{aligned} &\textit{(i) If } \kappa_1 \leq 0, \quad \Delta Y^*_{MSY}(D) < 0 \quad \textit{for all } D > 0, \\ &\textit{(ii) If } \kappa_1 > 0, \quad \begin{cases} \Delta Y^*_{MSY}(D) < 0, & \textit{if } D < -\dfrac{\kappa_0}{2\kappa_1}, \\ \Delta Y^*_{MSY}(D) = 0, & \textit{if } D = -\dfrac{\kappa_0}{2\kappa_1}, \\ \Delta Y^*_{MSY}(D) > 0, & \textit{if } D > -\dfrac{\kappa_0}{2\kappa_1}. \end{cases} \end{aligned}$$

Proof. If $\kappa_2 = 0$ and $\kappa_0 = 0$, then, $\Phi(D) = \kappa_1 D$, therefore, we deduce the three cases of the second item according to the sing of the parameter κ_1.
If $\kappa_0 > 0$ or $\kappa_0 < 0$, then, according to the sign of κ_1 we deduce the prove of the first and third items. □

Theorem 5.5. *Assume that $\kappa_2 < 0$ (resp. $\kappa_2 > 0$). We distinguish the following situations:*

1. *If $\kappa_1^2 \leq 4\kappa_0\kappa_2$, then $\Delta Y^*_{MSY}(D) \leq 0$ (resp. $\Delta Y^*_{MSY}(D) \geq 0$) for all D.*
2. *If $\kappa_1^2 > 4\kappa_0\kappa_2$, we consider the following cases:*

(a) If $\kappa_0 > 0$ (resp. $\kappa_0 < 0$), there exists $D_0 = \frac{-\kappa_1 - \sqrt{\kappa_1^2 - 4\kappa_0\kappa_1}}{2\kappa_2} > 0$, such that

$$\Delta Y^*_{MSY}(D) \begin{cases} < 0 & \text{if } D > D_0 \text{ (resp. } < D_0), \\ = 0 & \text{if } D = D_0, \\ > 0 & \text{if } D_0 < D \text{ (resp. } > D_0). \end{cases}$$

(b) If $\kappa_0 \leq 0$ (resp. $\kappa_0 \geq 0$):

(i) If $\kappa_1 < 0$ (resp. $\kappa_1 > 0$), then $\Delta Y^*_{MSY}(D) \leq 0$ (resp. $\Delta Y^*_{MSY}(D) \geq 0$) for all D.

(ii) If $\kappa_1 \geq 0$ (resp. $\kappa_1 \leq 0$), there exist two positive solutions:

$$D_1 = \frac{-\kappa_1 + \sqrt{\kappa_1^2 - 4\kappa_0\kappa_1}}{2\kappa_2} > 0, \quad D_2 = \frac{-\kappa_1 - \sqrt{\kappa_1^2 - 4\kappa_0\kappa_1}}{2\kappa_2} > 0.$$

Such that

$$\Delta Y^*_{MSY}(D) \begin{cases} < 0 & \text{if } D < D_1 \text{ and } D > D_2 \text{ (resp.} D_1 < D < D_2), \\ = 0 & \text{if } D = D_1 \text{ or } D = D_2, \\ > 0 & \text{if } D_1 < D < D_2 \text{ (resp.} D < D_1 \text{ and } D > D_2). \end{cases}$$

Proof. Assuming that $\kappa_2 < 0$ (resp. $\kappa_2 > 0$), we have the discriminant of this polynomial equal to $\kappa_1^2 - 4\kappa_0\kappa_2$). Thus, we analyze the sign of the discriminant, the number of solutions to $\Phi(D) = 0$, and the sign of these solutions in each case. This completes the proof of the theorem. □

As a corollary of the previous theorems, we obtain the following result:

Corollary 5.6. *The MSY of total yield for connected patches $Y^*_{MSY,T}(\infty)$ can be greater than the sum of yields associated with single isolated patches $Y^*_{MSY,T}(0)$, if one of the following conditions are satisfied:*

1. $\kappa_0 \geq 0, \kappa_1 \geq 0, \kappa_2 = 0,$
2. $\kappa_0 > 0, \kappa_1 < 0, \kappa_2 = 0, D < -\frac{\kappa_0}{2\kappa_1},$
3. $\kappa_0 < 0, \kappa_1 > 0, \kappa_2 = 0, D > -\frac{\kappa_0}{2\kappa_1},$
4. $\kappa_0 > 0, \kappa_1^2 > 4\kappa_0\kappa_2, \kappa_2 < 0, D < \frac{-\kappa_1 + \sqrt{\kappa_1^2 - 4\kappa_0\kappa_1}}{2\kappa_2},$
5. $\kappa_0 \leq 0, \kappa_1 > 2\sqrt{\kappa_0\kappa_2}, \kappa_2 < 0,$ *and* $\frac{-\kappa_1 + \sqrt{\kappa_1^2 - 4\kappa_0\kappa_1}}{2\kappa_2} < D < \frac{-\kappa_1 + \sqrt{\kappa_1^2 - 4\kappa_0\kappa_1}}{2\kappa_2}.$
6. $\kappa_2 > 0, \kappa_1^2 \leq 4\kappa_0\kappa_2,$
7. $\kappa_0 < 0, \kappa_1^2 > 4\kappa_0\kappa_2, \kappa_2 > 0, D > \frac{-\kappa_1 + 2\sqrt{\kappa_1^2 - 4\kappa_0\kappa_1}}{2\kappa_2},$
8. $\kappa_0 \geq 0, \kappa_1 > 0, \kappa_2 > 0,$
9. $\kappa_0 \geq 0, \kappa_1 \leq 2\sqrt{\kappa_0\kappa_2}, \kappa_2 > 0,$ *and* $\frac{-\kappa_1 + \sqrt{\kappa_1^2 - 4\kappa_0\kappa_1}}{2\kappa_2} > D$ *and* $D > \frac{-\kappa_1 + \sqrt{\kappa_1^2 - 4\kappa_0\kappa_1}}{2\kappa_2}.$

Proof. This is a direct consequence of Theorems 5.4 and 5.5. □

6. Two-patch case

In this part, we focus on the two-patch Holling type II predator–prey model (3.1) with $n = 2$, where the prey and its predator can move from one fishing area to another. We assume that condition H is satisfied, *i.e.*,

$\gamma_{12} = \gamma_{21}$ and $D_1 = D_2$. The complete model reads as follows:

$$\begin{cases} \dfrac{\mathrm{d}x_1}{\mathrm{d}t} = r_1 x_1 \left(1 - \dfrac{x_1}{K_1}\right) - \dfrac{a_1 x_1 y_1}{x_1 + D} + \epsilon(x_2 - x_1), \\ \dfrac{\mathrm{d}x_2}{\mathrm{d}t} = r_2 x_2 \left(1 - \dfrac{x_2}{K_2}\right) - \dfrac{a_2 x_2 y_2}{x_2 + D} + \epsilon(x_1 - x_2), \\ \dfrac{\mathrm{d}y_1}{\mathrm{d}t} = \left(\dfrac{e a_1 x_1}{x_1 + D} - d_1\right) y_1 - E_1 y_1 + \epsilon(\theta y_2 - y_1), \\ \dfrac{\mathrm{d}y_2}{\mathrm{d}t} = \left(\dfrac{e a_2 x_2}{x_2 + D} - d_2\right) y_2 - E_2 y_2 + \epsilon(y_1 - \theta y_2), \end{cases} \tag{6.1}$$

where θ denote θ_{12}/θ_{21}. Note that the system (6.1) is homogeneous if and only if $r_1 = r_2$, $K_1 = K_2$, and $a_1 = a_2$. Our aim here is to find the conditions on (6.1) such that the excess yield (5.6) is positive as a function of the asymmetry in predator migration.

The total Yield Y_T^* reads as follows:

$$Y_T^*(\epsilon, E_1, E_2) = e\left(r_1\, x_1^* \left(1 - \frac{x_1^*}{K_1}\right) + r_2\, x_2^* \left(1 - \frac{x_2^*}{K_2}\right)\right) - d_1\, y_1^* - d_2\, y_2^*, \tag{6.2}$$

where $(x_1^*, x_2^*; y_1^*, y_2^*)$ denotes the equilibrium point of (6.1), which is assumed to depend on the migration rate ϵ and the fishing efforts E_1 and E_2. For $\epsilon = 0$, the sum of the MSY of each isolated patch, defined by $Y_{MSY,T}^*(0) = \max_{(E_1,E_2)} Y_T^*(0, E_1, E_2)$, takes the following form:

$$Y_{MSY,T}^*(0) = \frac{1}{4}\left(\frac{r_1}{a_1 K_1}\frac{(K_1(ea_1 - d_1) - d_1 D)^2}{ea_1 - d_1} + \frac{r_2}{a_2 K_2}\frac{(K_2(ea_2 - d_2) - d_2 D)^2}{ea_2 - d_2}\right), \tag{6.3}$$

where $ea_i - d_i > 0$ for all i, and in the case when ϵ approaches infinity, after reduction, the reduced model (4.2) reads as follows:

$$\begin{cases} \dfrac{dX}{\mathrm{d}t} = rX\left(1 - \dfrac{X}{K}\right) - a\dfrac{XY}{X + 2D}, \\ \dfrac{dY}{\mathrm{d}t} = \left(ea\dfrac{X}{X + 2D} - \mathrm{d}\right)Y - EY, \end{cases} \tag{6.4}$$

where

$$r = \frac{r_1 + r_2}{2}, \quad K = 2\frac{r_1 + r_2}{\alpha_1 + \alpha_2}, \quad d = \frac{\theta d_1 + d_2}{\theta + 1}, \quad E = \frac{\theta E_1 + E_2}{\theta + 1}, \text{ and } a = \frac{\theta a_1 + a_2}{\theta + 1}. \tag{6.5}$$

Thus, the reduced model (6.4) admits (X^*, Y^*) with

$$(X^*(E), Y^*(E)) = \left(\frac{2D(d + E)}{ea - d - E}, \frac{2rD}{a}\left(1 + \frac{d + E}{ea - d - E}\right)\left(1 - \frac{2D(d + E)}{K(ea - d - E)}\right)\right),$$

as a positive equilibrium. Therefore, $Y_{MSY,T}^*(\infty, \theta)/ = \max_E Y_T^*(\infty, E)$, and after simplification, we obtain for any $\theta > 0$:

$$Y_{MSY,T}^*(\infty, \theta) = \frac{1}{4}\frac{\vartheta_2\theta^2 + \vartheta_1\theta + \vartheta_0}{\omega_2\theta^2 + \omega_1\theta + \omega_0}, \tag{6.6}$$

where ω_i and ϑ_i are given by:

$$\begin{cases} \vartheta_0 = (-K_1\,K_2\,r_1\,ea_2 + Dd_2\,r_1\,K_2 + K_1\,K_2\,r_1\,d_2 - K_1\,K_2\,r_2\,ea_2 + K_1\,K_2\,r_2\,d_2 + Dd_2\,r_2\,K_1)^2\,, \\ \vartheta_1 = 2\,(-K_1\,K_2\,r_1\,ea_2 + Dd_2\,r_1\,K_2 + K_1\,K_2\,r_1\,d_2 - K_1\,K_2\,r_2\,ea_2 + K_1\,K_2\,r_2\,d_2 + Dd_2\,r_2\,K_1) \\ \times\,(-K_1\,K_2\,r_1\,ea_1 - K_1\,K_2\,r_2\,ea_1 + K_1\,K_2\,r_1\,d1 + Dd_1\,r_1\,K_2 + Dd_1\,r_2\,K_1 + K_1\,K_2\,r_2\,d_1)\,, \\ \vartheta_2 = (-K_1\,K_2\,r_1\,ea_1 - K_1\,K_2\,r_2\,ea_1 + K_1\,K_2\,r_1\,d1 + Dd_1\,r_1\,K_2 + Dd_1\,r_2\,K_1 + K_1\,K_2\,r_2\,d_1)^2\,, \\ \omega_0 = (ea_2 - d_2)\,K_2\,K_1\,a_2\,\,(r_1\,K_2 + r_2\,K_1)\,, \\ \omega_1 = ((ea_2 - d_2)\,K_2\,K_1\,a_1 + (ea_1 - d_1)\,K_2\,K_1\,a_2)\,(r_1\,K_2 + r_2\,K_1)\,, \\ \omega_2 = (ea_1 - d_1)\,K_2\,K_1\,a_1\,\,(r_1\,K_2 + r_2\,K_1)\,. \end{cases} \tag{6.7}$$

Note that ϑ_0, ϑ_2 are non negative and $\omega_i > 0$ for all i since $ea_i - d_i > 0$ by hypothesis.

The condition to have a positive excess yield $\Delta Y^*_{MSY,T}(\theta)$ simplify to:

$$\frac{\vartheta_2\theta^2 + \vartheta_1\theta + \vartheta_0}{\omega_2\theta^2 + \omega_1\theta + \omega_0} > \frac{r_1}{a_1K_1}\frac{(K_1(ea_1 - d_1) - d_1D)^2}{ea_1 - d_1} + \frac{r_2}{a_2K_2}\frac{(K_2(ea_2 - d_2) - d_2D)^2}{ea_2 - d_2}.$$

Now, we will analyze the effect of predator dispersal asymmetry on the excess yield. For this purpose, we focus on the two-patch model (6.1) with the following parameter values: $r_1 = 1$, $r_2 = 2$, $K_1 = 2$, $K_2 = 3$, $a_1 = 1$, $a_2 = 2$, $e = 1$, $d_1 = \frac{1}{2}$, $d_2 = \frac{1}{2}$, and $D = 1$. For this set of parameters, (6.3) and (6.6) simplify to:

$$Y^*_{MSY,T}(0) = \frac{49}{72}$$

and

$$Y^*_{MSY,T}(\infty, \theta) = \frac{1}{336}\frac{(11\theta + 47)^2}{(\theta + 3)(\theta + 2)}.$$

Consequently, the excess yield $\Delta Y^*_{MSY,T}(\theta)$ is given by:

$$\Delta Y^*_{MSY,T}(\theta) = -\frac{1}{1008}\frac{323\theta^2 + 328\theta - 2511}{(\theta + 3)(\theta + 2)}.$$

Therefore, the excess satisfied to:

$$\Delta Y^*_{MSY,T}(\theta) \begin{cases} > 0 & \text{if} \quad 0 < \theta < -\frac{164}{323} + \frac{49}{323}\sqrt{349}, \\ = 0 & \text{if} \quad \theta = -\frac{164}{323} + \frac{49}{323}\sqrt{349}, \\ < 0 & \text{else.} \end{cases} \tag{6.8}$$

The previous example shows that the dispersal asymmetry of the predator can lead the yield to become positive and decrease as θ increases. Furthermore, for the symmetric case, *i.e.*, with $\theta = 1$, the excess yield at the MSY is equal to $\frac{155}{1008}$. In Figure 3, the graph of the function $\Delta Y^*_{MSY,T}(\theta)$ is shown in blue, as a function of the asymmetric migration of the predator for $\theta \in (0, 5]$.

7. Numerical simulations

As shown in the previous Subsections 5 and 6, in general, it is very difficult to calculate explicitly the formula for the yield Y_i^* of each patch and, consequently, the total yield $\sum_i Y_i^*$ for the connected n-patch model (3.1), except in special cases, such as in Proposition 5.1 for $\epsilon = 0$ and when $\epsilon \to \infty$. In this section, we present some numerical results comparing $Y^*_{MSY,T}(\infty)$ and $Y^*_{MSY,T}(0)$ for two and three patches.

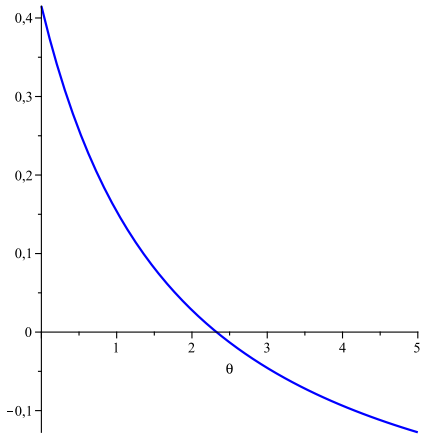

FIGURE 3. The graph of $\Delta Y^*_{MSY,T}(\theta)$ for $r_1 = 1, r_2 = 2, K_1 = 2, K_2 = 3, a_1 = 1, a_2 = 2, e = 1, d_1 = 1/2, d_2 = 1/2, D = 1$ and when $\theta \in]0, 5]$.

TABLE 1. Parameter values for the two-patch model (6.1) used in Figures 4, 5, 6, and 7.

Figures	r_1	r_2	K_1	K_2	a_1	a_2	d_1	d_2	D	e	θ
Figures 4 and 5	1	1	1	1	8	8	1	1	1	2	1
Figures 6 and 7	2	1	0.5	0.7	6	0.5	0.5	1	1	5	4

7.1. Example of two-patch model

We propose in this part to provide some examples of the total yield $Y^*_T(\epsilon, E_1, E_2)$ as a function of the fishing efforts E_1 and E_2, for a fixed migration rate ϵ. Our aim is to illustrate and confirm the results of Subsection 5.1, as well as to demonstrate through an example that the excess yield $\Delta Y^*_{MSY,T}$ can be positive (see Subsection 5.2). We consider the two-patch model (6.1). We plot the total yield $Y^*_T(\epsilon, E_1, E_2) = (Y^*_1 + Y^*_2)(\epsilon, E_1, E_2)$ with respect to the fishing efforts E_1 and E_2, along with projections onto the planes $E_1 = 0$ and $E_2 = 0$, for $\epsilon = 0$ and $\epsilon \to \infty$. The total yield $Y^*_T(\epsilon, E_1, E_2)$ and these projections are shown in green, while the plane $Y^*_T = Y^*_{MSY}(0)$ given in (6.3) is shown in blue in all the figures.

In Table 2, we compute the yield excess $\Delta Y^*_{MSY,T}(\epsilon)$ given by the following formula:

$$\Delta Y^*_{MSY,T}(\epsilon) = Y^*_{MSY,T}(\epsilon) - Y^*_{MSY,T}(0), \tag{7.1}$$

and the percentage of yield excess defined as:

$$\%\Delta Y^*_{MSY,T}(\epsilon) = 100 \left| \frac{\Delta Y^*_{MSY,T}(\epsilon)}{Y^*_{MSY,T}(\epsilon)} \right|. \tag{7.2}$$

Figures 4, 5, and Table 2, for the set of parameters given in the first line of Table 1, confirm the result proven in Subsection 5.1 when considering two homogeneous patches. In this case, the excess yield is equal to zero. This result can be observed geometrically in Figure 5a and in the projections shown in Figures. 5b and 5c. Specifically, the surface is always below the blue plane, which represents the tangent space of this surface at the point $(E^*_{MSY,1}, E^*_{MSY,2})$, where the yield is maximal.

TABLE 2. Values of $Y^*_{MSY,T}$ and $\Delta Y^*_{MSY,T}$ were obtained for the parameters given in Table 1, for migration rates $\epsilon = 0$ and ϵ close to ∞. The parameters in the first row of Table 1 correspond to Figures 4 and 5, while the parameters in the second row correspond to Figures 6 and 7.

Case	Figure	ϵ	$Y^*_{MSY,T}(\epsilon)$	$(\Delta Y^*_{MSY,T})(\epsilon)$	$\%\Delta Y^*_{MSY,T}$
Homogeneous	Figure 4	0	0.81	+0.00	00.00%
	Figure 5	∞	0.81	+0.00	00.00%
Heterogeneous	Figure 6	0	1.15	+0.00	00.00%
	Figure 7	∞	1.85	+0.70	37.83%

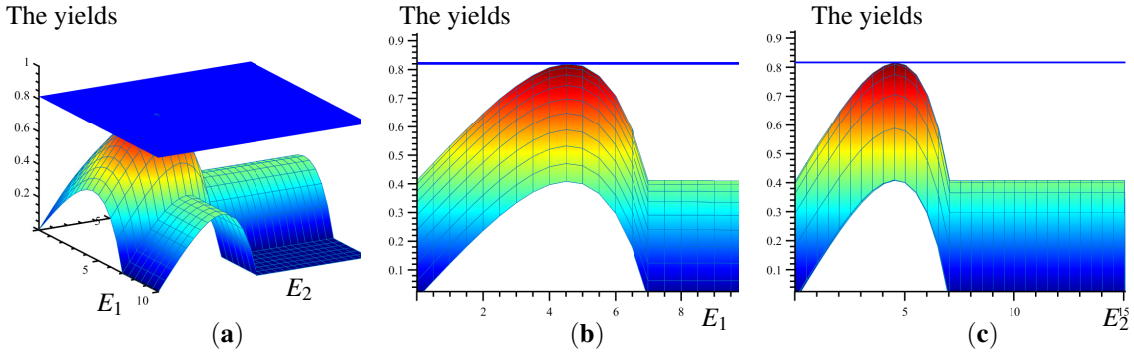

FIGURE 4. Case a: The total yield $Y^*_T(0, E_1, E_2) = (Y^*_1 + Y^*_2)(0, E_1, E_2)$ with respect to the fishing efforts $E_1 \in [0, 10]$ and $E_2 \in [0, 15]$. The total yield $Y^*_T = Y^*_{MSY}(0)$ given in (6.3) is shown in blue for the parameter set provided in the first line of Table 1 and the migration rate $\epsilon = 0$. Case b (resp. c): The projection of the total yields $Y^*_T(0, E_1, E_2)$ and $Y^*_T = 0.81$ onto the plane $E_1 = 0$ (resp. $E_2 = 0$).

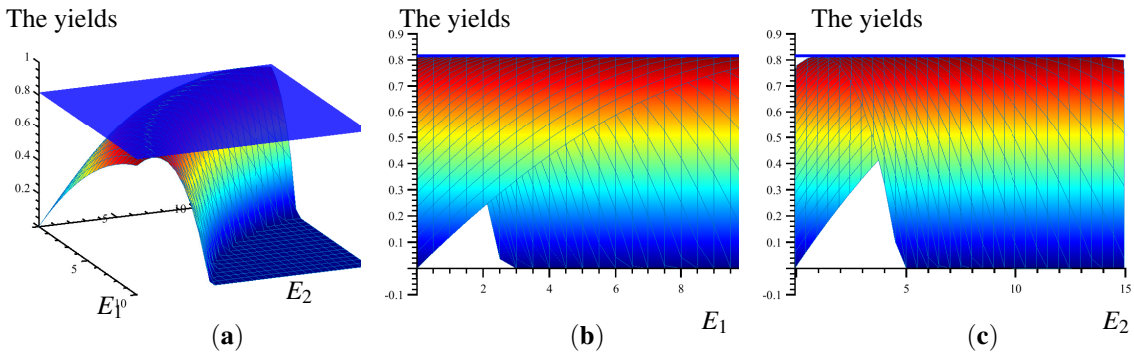

FIGURE 5. Case a: The total yield $Y^*_T(\infty, E_1, E_2) = (Y^*_1 + Y^*_2)(\infty, E_1, E_2)$ with respect to the fishing efforts $E_1 \in [0, 10]$ and $E_2 \in [0, 15]$, and the total yield $Y^*_T = Y^*_{MSY}(0)$ given in (6.3) is shown in blue for the sets of the parameter given in the first line of Table 1 and the migration rate ϵ tend to ∞. Case b (resp. c): the projection of the total yields $Y^*_T(0, E_1, E_2)$ and $Y^*_T = 0.81$ in the plan $E_1 = 0$ (resp. $E_2 = 0$).

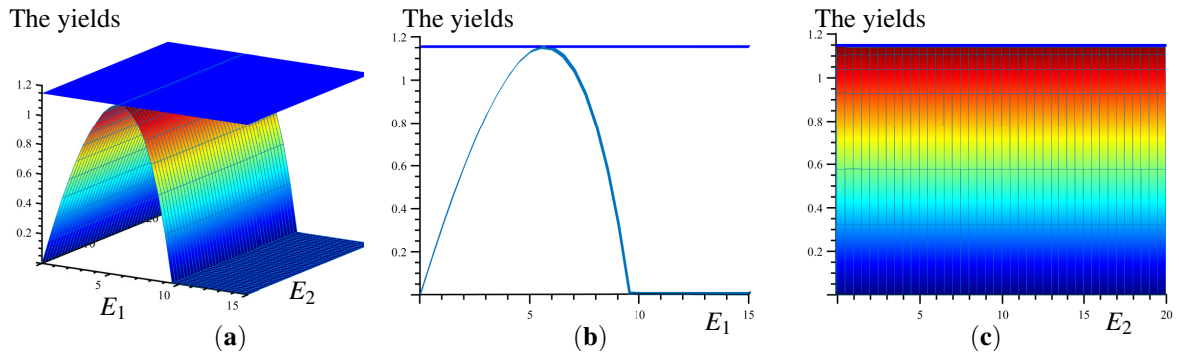

FIGURE 6. Case a: The total yield $Y_T^*(0, E_1, E_2) = (Y_1^* + Y_2^*)(0, E_1, E_2)$ with respect to the fishing efforts $E_1 \in [0, 15]$ and $E_2 \in [0, 20]$, and the total yield $Y_T^* = Y_{MSY}^*(0)$ given in (6.3) is shown in blue for the sets of the parameter given in the second line of Table 1 and the migration rate ϵ equal to 0. Case b (resp. c): the projection of the total yields $Y_T^*(0, E_1, E_2)$ and $Y_T^* = 1.15$ in the plan $E_1 = 0$ (resp. $E_2 = 0$).

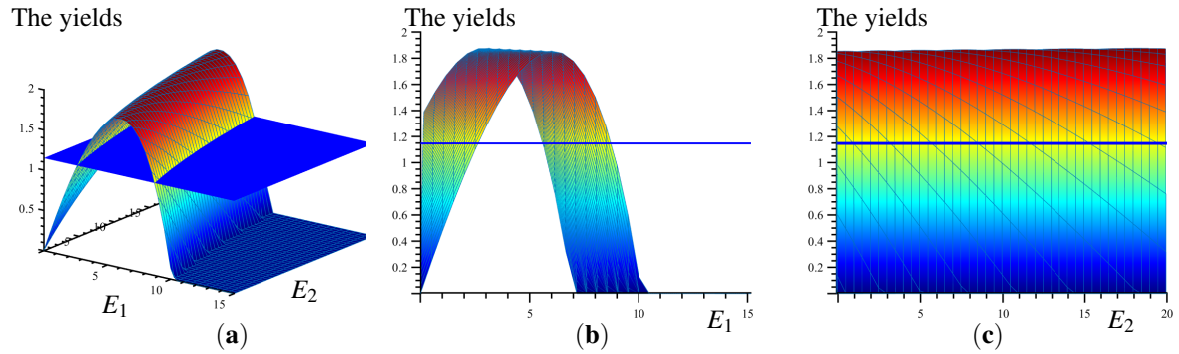

FIGURE 7. Case a: The total yield $Y_T^*(\infty, E_1, E_2) = (Y_1^* + Y_2^*)(\infty, E_1, E_2)$ with respect to the fishing efforts $E_1 \in [0, 15]$ and $E_2 \in [0, 20]$, and the total yield $Y_T^* = Y_{MSY}^*(0)$ given in (6.3) is shown in blue for the sets of the parameter given in the second line of Table 1 and the migration rate ϵ tend to ∞. Case b (resp. c): the projection of the total yields $Y_T^*(0, E_1, E_2)$ and $Y_T^* = 1.15$ in the plan $E_1 = 0$ (resp. $E_2 = 0$).

TABLE 3. Parameter values used in Figures 8a, 8b, 8c and 8d.

Figure	r_1	r_2	r_3	K_1	K_2	K_3	a_1	a_2	a_3	d_1	d_2	d_3	e
Figure 8a	11	2	12	1.1	2.1	1	1	12	1.3	0.7	1	1	1.7
Figure 8b	1	2	12	1	2.1	1	1	2	3	1	1	1	3
Figure 8c	1	2	12	1	21	1	0.2	2	3	1	1	1	1
Figure 8d	1	2	3	1	2	1.1	0.2	2	3	1	1	0.1	1

Figures 6, 7, and Table 2 compare the total yields obtained for isolated and coupled patches in the case of two heterogeneous patches, using the set of parameters given in the second line of Table 1. These figures confirm the result proven in Subsection 5.2. The analysis demonstrates that, within a specific range of fishing efforts, the total yield for the coupled patches can exceed the sum of the yields from the isolated patches.

TABLE 4. Values of $\kappa_0, \kappa_1, \kappa_2$ and $\kappa_1^2 - 4\kappa_0\kappa_1$ are obtained for the parameter set given in Table 3.

Figure	κ_0	κ_1	κ_2	$\kappa_1^2 - 4\kappa_0\kappa_1$	D_0	D_1	D_2
Figure 8a	+2.77	+23.28	−28.06	853.48	0.93	/	/
Figure 8b	−1.04	+05.25	−02.11	018.17	/	0.21	2.26
Figure 8c	−4.53	+10.67	+12.03	327.23	0.30	/	/
Figure 8d	+0.83	+07.93	−13.25	018.61	/	/	/

7.2. Illustration results of Corollary 5.6 for three-patch model

In this subsection, we present numerical examples to illustrate the results stated in Corollary 5.6 for the three-patch model, as follows:

$$\begin{cases} \dfrac{\mathrm{d}x_1}{\mathrm{d}t} = r_1 x_1 \left(1 - \dfrac{x_1}{K_1}\right) - \dfrac{a_1 x_1 y_1}{x_1 + D} + \epsilon(-2x_1 + x_2 + x_3), \\ \dfrac{\mathrm{d}x_2}{\mathrm{d}t} = r_2 x_2 \left(1 - \dfrac{x_2}{K_2}\right) - \dfrac{a_2 x_2 y_2}{x_2 + D} + \epsilon(x_1 - 2x_2 + x_3), \\ \dfrac{\mathrm{d}x_3}{\mathrm{d}t} = r_3 x_3 \left(1 - \dfrac{x_3}{K_3}\right) - \dfrac{a_3 x_3 y_3}{x_3 + D} + \epsilon(x_1 + x_2 - 2x_3), \\ \dfrac{\mathrm{d}y_1}{\mathrm{d}t} = \left(\dfrac{e a_1 x_1}{x_1 + D} - d_1\right) y_1 - E_1 y_1 + \epsilon(-2y_1 + y_2 + y_3), \\ \dfrac{\mathrm{d}y_2}{\mathrm{d}t} = \left(\dfrac{e a_2 x_2}{x_2 + D} - d_2\right) y_2 - E_2 y_2 + \epsilon(y_1 - 2y_2 + y_3), \\ \dfrac{\mathrm{d}y_3}{\mathrm{d}t} = \left(\dfrac{e a_3 x_3}{x_3 + D} - d_3\right) y_3 - E_3 y_3 + \epsilon(y_1 + y_2 - 2y_3). \end{cases} \tag{7.3}$$

In the Table 4 we compute the values of $\kappa_0, \kappa_1, \kappa_2, \kappa_1^2 - 4\kappa_0\kappa_1$ and D_i for the parameters given in Table 3. In Figures 8a, 8b, 8c and 8d, we plot the curve of the function Φ as the parameter D varies from 0 to ∞.

8. Concluding remarks

In this study, we investigated a metapopulation model with predator–prey interactions to compare the Maximum Sustainable Yield (MSY) under two extreme scenarios: isolated patches and connected patches with rapid fish movement.

In the case where predators are harvested in a homogeneous environment with identical parameters across all patches and symmetric movement between patches, we demonstrated that the yield at MSY for the interconnected system is equal to the sum of the yields from the isolated patches.

We then explored the heterogeneous case, where patches have distinct parameters. This analysis showed that such differences can result in scenarios where the yield at MSY for the interconnected system is greater than, equal to, or less than the sum of the yields from isolated patches. To illustrate these concepts concretely, we provided a specific example with two patches.

A limitation of this work comes from the hypothesis **H** considering all predation parameters D similar and a symmetric migration matrix for the prey. This hypothesis makes it possible to obtain a reduced model similar to local models, that is to say the RM model. Recall that in [8] the general case without the **H** hypothesis for two connected patches was treated. in this work it was shown that the reduced model was no longer the RM model but that there could be a positive excess yield. One perspective remains to study the general case with any number of patches but without hypothesis **H**.

This work has other limitations, particularly regarding its application to real fisheries. We have shown that heterogeneity between sites makes it possible to obtain a positive and relatively high excess yield. However, in the

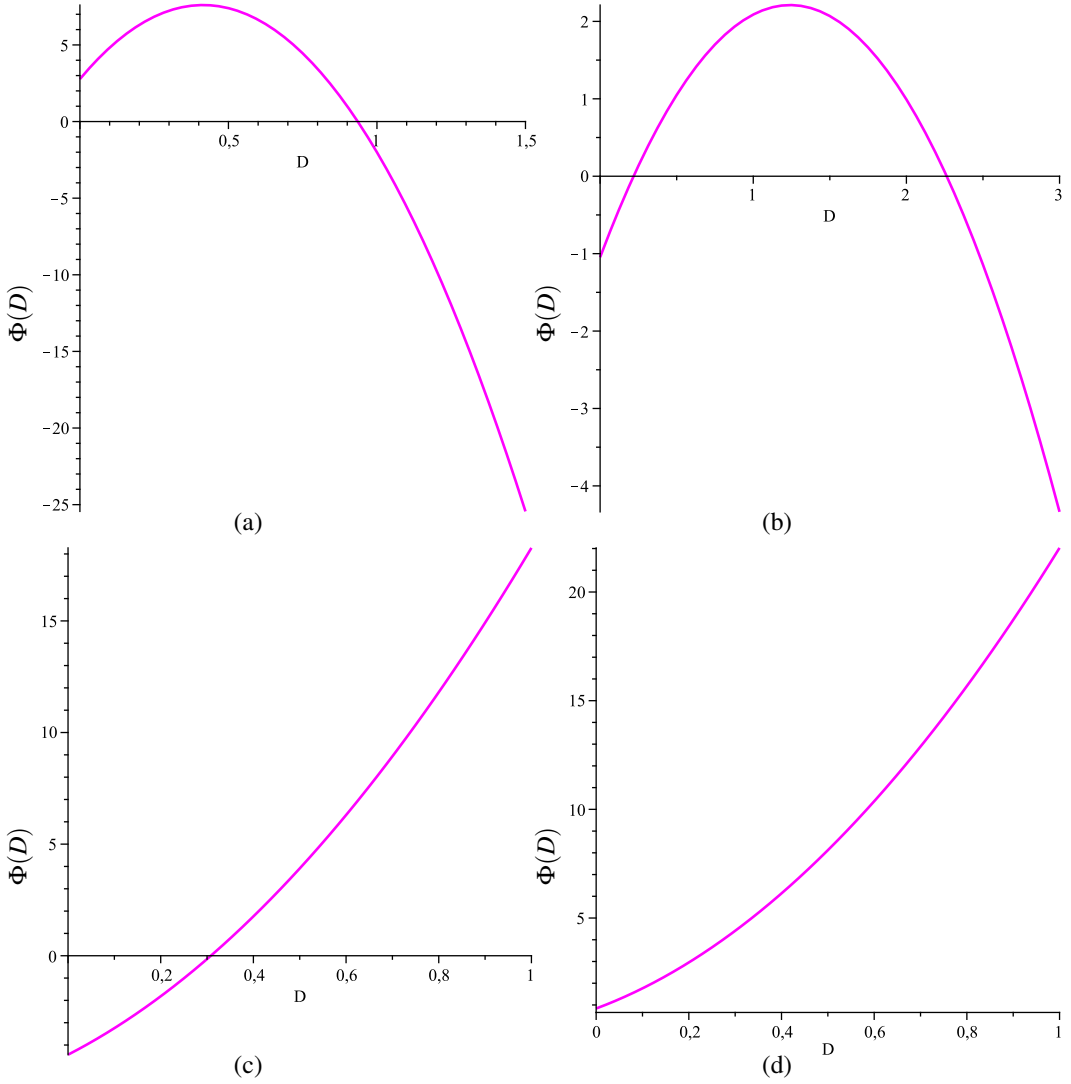

FIGURE 8. The curve of the function Φ given by (5.11) for the parameters given in the Tables 3 and 4.

real world, it is difficult to be able to modify the environmental characteristics of the various connected sites. One of the parameters on which we can play to a certain extent is the surface area of the sites and consequently their carrying capacity. Indeed, if we assume that the resource density of the prey fish is homogeneous in each site, the carrying capacity of a site should be proportional to the size of the site. To apply the method, it is therefore useful to consider to establish connections between sites of different sizes. We can also consider modifying prey fish predation rates by installing artificial habitats in certain sites. The creation of these habitats or artificial reefs should make it possible to create refuge areas where prey fish are protected from predator attacks and consequently reduce predation rates.

In the future, we plan to collaborate with marine biologists and fisheries scientists to explore a controlled environment, with potential real-world applications, particularly in the field of aquaculture involving connected breeding ponds.

Data availability statement

No new data/codes were created or analyzed in this study.

References

[1] B. Elbetch, T. Benzekri, D. Massart and T. Sari, The multi-patch logistic equation. *Discrete Continuous Dyn. Syst. Ser. B* **26** (2020) 6405–6424.

[2] B. Elbetch, T. Benzekri, D. Massart and T. Sari, The multi-patch logistic equation with asymmetric migration. *Rev. Integr. Temas Mater.* **40** (2022) 25–57.

[3] B. Elbetch, Effect of dispersal in Two-patch environment with Richards growth on population dynamics. *J. Innov. Appl. Math. Comput. Sci.* **2** (2022) 41–68.

[4] B. Elbetch and A. Moussaoui, Nonlinear diffusion in the multi-patch logistic model. *J. Math. Biol.* **87** (2023) 1–32.

[5] B. Elbetch, Effect of dispersal in single-species discrete diffusion systems with source-sink patches. *Math. Appl.* **51** (2023) 51–97.

[6] B. Elbetch, Effects of rapid population growth on total biomass in Multi-patch environment. *Differ. Equ. Appl.* **15** (2023) 323–359.

[7] B. Elbetch, Generalized logistic equation on networks. *Comptes Rendus Math.* **361** (2023) 911–934.

[8] P. Auger, B. Kooi and A. Moussaoui, Increase of maximum sustainable yield for fishery in two patches with fast Migration. *Ecol. Model.* **467** (2022) 109898.

[9] R. Arditi, C. Lobry and T. Sari, In dispersal always beneficial to carrying capacity? New insights from the multi-patch logistic equation. *Theor. Popul. Biol.* **106** (2015) 45–59.

[10] R. Arditi, C. Lobry and T. Sari, Asymmetric dispersal in the multi-patch logistic equation, *Theor. Popul. Biol.* **120** (2018) 11–15.

[11] D.L. DeAngelis, C.C. Travis and W.M. Post, Persistence and stability of seed-dispersel species in a patchy environment. *Theor. Popul. Biol.* **16** (1979) 107–125.

[12] D.L. DeAngelis and B. Zhang, Effects of dispersal in a non-uniform environment on population dynamics and competition: a patch model approach. *Discrete Contin. Dyn. Syst. Ser. B* **19** (2014) 3087–3104.

[13] D.L. DeAngelis, W.-M. Ni and B. Zhang, Effects of diffusion on total biomass in heterogeneous continuous and discrete-patch systems. *Theor. Ecol.* **9** (2016) 443–453.

[14] H.I. Freedman and P. Waltman, Mathematical models of population interactions with dispersal. I. Stability of two habitats with and without a predator. *SIAM J. Appl. Math.* **32** (1977) 631–648.

[15] H.I. Freedman and Y. Takeuchi, Global stability and predator dynamics in a model of prey dispersal in a patchy environment. *Nonlinear Anal. Theory Methods Appl.* **13** (1989) 993–1002.

[16] J.-C. Poggiale, P. Auger, D. Nerini, C. Manté and F. Gilbert, Global production increased by a spatial heterogeneity in a population dynamics model. *Acta Biotheoretica* **53** (2005) 359–370.

[17] J. Arino, N. Bajeux and S. Kirkland, Number of source patches required for population persistence in a source-sink metapopulation with explicit movement. *Bull. Math. Biol.* **81** (2019) 1916–1942.

[18] H. Wu, Y. Wang, Y. Li and D.L. DeAngelis, Dispersal asymmetry in a two-patch system with source-sink populations. *Theor. Popul. Biol.* **131** (2019) 54–65.

[19] D. Gao , How does dispersal affect the infection size? *SIAM J. Appl. Math.* **80** (2020) 2144–2169.

[20] D. Gao and S. Ruan, A multipatch malaria model with logistic growth. *SIAM J. Appl. Math.* **72** (2012) 819–841.

[21] D. Gao and C.P. Dong, Fast diffusion inhibits disease outbreak. *Proc. Am. Math. Soc.* **148** (2020) 1709–1722.

[22] M. Benaim, C. Lobry, T. Sari and E. Strickler. When can a population spreading across sink habitats persist ? *J. Math. Biol.* **88** (2024) 19.

[23] M. Benaim, C. Lobry, T. Sari and E. Strickler, Untangling the role of temporal and spatial variations in persistence of populations. *Theor. Popul. Biol.* **154** (2023) 1–26.

[24] G. Katriel, Dispersal-induced growth in a time-periodic environment. *J. Math. Biol.* **85** (2022) 24.

[25] P. Auger, C. Lett, A. Moussaoui and S. Pioch, Optimal number of sites in artificial pelagic multisite fisheries. *Can. J. Fisher. Aquat. Sci.* **67** (2010) 296–303.

[26] M. Bensenane, A. Moussaoui and P. Auger, On the optimal size of marine reserves. *Acta Biotheoretica* **61** (2013) 109–118.

[27] R. Hilborn, F. Michel and G.A. DeLeo, Integrating marine protected areas with catch regulation. *Can. J. Fisher. Aquat. Sci.* **63** (2006) 642–649.

[28] A. Moussaoui, M. Bensenane, P. Auger and A. Bah, On the optimal size and number of reserves in a multi-site fishery model. *J. Biol. Syst.* **22** (2014) 1–17.

[29] A. Moussaoui, P. Auger and C. Lett, Optimal number of sites in multi-site fisheries with fish stock dependent migrations. *Math. Biosci. Eng.* **8** (2011) 769–783.

[30] B. Elbetch and A. Moussaoui, Enhancing maximum sustainable yield in a patchy prey–predator environment. *Ecol. Complex.* **60** (2024) 101107.

[31] C.W. Clark, Mathematical Bioeconomis. The Optimal Management of Renewable Resources. 2nd edn. John Wiley and Sons, Inc., New York (1990).

[32] D. Nguyen Ngoc, T. Nguyen Huu and P. Auger, Connectivity between two fishing sites can lead to an emergence phenomenon related to Maximum Sustainable Yield. *J. Theor. Biol.* **595** (2024) 111913.

[33] R. Bravo de la Parra, J.-C. Poggiale and P. Auger, The effect of connecting sites in the environment of a harvested population. *Math. Model. Nat. Phenom.* **18** (2023).

[34] A.N. Tikhonov, Systems of differential equations containing small parameters in the derivatives. *Mat. Sb. (N.S.)* **31** (1952) 575–586.

[35] W.R. Wasow, Asymptotic Expansions for Ordinary Differential Equations, Robert E. Krieger Publishing Company, Huntington, NY (1976).

[36] H.I. Freedman, Deterministic Mathematical Models in Population Ecology. M. Dekker, New York (1980).

[37] M. Kot, Elements of Mathematical Ecology. Cambridge University Press (2001).

[38] S.B. Hsu, S.P. Hubbell and P. Waltman, Competing predators. *SIAM J. Appl. Math.* **35** (1978) 617–625.

[39] K.S. Cheng, Uniqueness of a limit cycle for a predator–prey system. *SIAM J. Math. Anal.* **12** (1981) 541–548.

[40] L.P. Liou and K.S. Cheng, On the uniqueness of a limit cycle for a predator–prey system. *SIAM J. Math. Anal.* **19** (1988) 867–878.

[41] B. Ghosh, T.K. Kar and T. Legovic, Relationship between exploitation, oscillation, MSY and extinction. *Math. Biosci.* **256** (2014) 1–9.

[42] H.I. Freedman, Deterministic Mathematical Models in Population Ecology, Marcel Dekker, New York (1980).

[43] Y. Kuang and Y. Takeuchi, Predator–prey dynamics in models of prey dispersal in two-patch environments. *Math. Biosci.* **120** (1994) 77–98.

[44] H.L. Smith and P. Waltman, The Theory of the Chemostat. Cambridge Studies in Mathematical Biology (1995).

[45] P. Auger, R. Bravo de la Parra, J.-C. Poggiale, E. Sánchez and T. Nguyen Huu, Aggregation of variables and applications to population dynamics, in Structured Population Models in Biology and Epidemiology. Lecture Notes in Mathematics, Vol. 1936, edited by P. Magal, S. Ruan. Math. Biosci. Subseries. Springer, Berlin (2008) 209–263.

[46] P. Auger, R. Bravo de la Parra, J.C. Poggiale, E. Sánchez and L. Sanz, Aggregation methods in dynamical systems and applications in population and community dynamics. *Phys. Life. Rev.* **5** (2008) 79–105.

[47] R. Kon and D. Kumar, Stability of Rosenzweig–MacArthur models with non-diffusive dispersal on non-regular networks. Theor. Popul. Biol. **150** (2023) 14–22.

[48] C. Cosner, J.C. Beier, R.S. Cantrell, D. Impoinvil, L. Kapitanski, M.D. Potts, A. Troyo and S. Ruan, The effects of human movement on the persistence of vector-borne diseases. *J. Theoret. Biol.* **258** (2009) 550–560.

[49] H. Guo, M.Y. Li and Z. Shuai, Global stability of the endemic equilibrium of multigroup SIR epidemic models. *Can. Appl. Math. Quart.* **14** (2006) 259–284.

[50] T. Legovic, J. Klanjscek and S. Gecek, Maximum sustainable yields and species extinction in ecosystems. *Ecol. Model.* **221** (2011) 1569–1574.

[51] M.L. Rosenzweig, Paradox of enrichment: destabilization of exploitation ecosystems in ecological time. *Science* (1971) 385–387.

[52] M.L. Rosenzweig, R.H. MacArthur, Graphical representation and stability conditions of predator–prey interactions. *Am. Naturalist* **97** (1963) 209–223.

[53] M.B. Schaefer, Some considerations of population dynamics and economics in relation to the management of the commercial marine fisheries. *J. Fish. Res. Board Canada* **14** (1957) 669–681.

Appendix A. Properties of the matrices of migration

Note that the matrices the matrices Γ and Θ combine the connection matrices derived from the patch graph and a description of the intensity of the connections. The connection matrix of the graph can be easily reconstructed from Γ (resp. Θ) by setting diagonal entries in Γ (resp. Θ) to zero and nonzero off-diagonal entries to 1. It is important to recall that if Γ (resp. Θ) is irreducible, then 0 is a simple eigenvalue of Γ (resp. Θ), and all non-zero eigenvalues of Γ (resp. Θ) have a negative real part. Furthermore, the kernel of the matrix Γ (resp. Θ) is generated by a positive vector (see Lemma 2 in [17]). Throughout this section, we denote this positive vector as $\delta := (\delta_1, \dots, \delta_n)^T$ (resp. $\xi := (\xi_1, \dots, \xi_n)^T$). For the existence, uniqueness, and positivity of δ (resp. ξ), refer to Lemma 1 of Cosner *et al.* [48], Lemma 4.1, and Lemma 1 of Elbetch *et al.* [1, 2]. Notably, if the matrix Γ (resp. Θ) is symmetric, then $\ker\Gamma$ (resp. $\ker\Theta$) is generated by $\delta = (1, \dots, 1)^T$ (resp. ξ). Additionally, it is shown in Guo *et al.* [49], Lemma 2.1 and Gao and Dong [21], Lemma 3.1 that the vector $(\Gamma^*_{11}, \dots, \Gamma^*_{nn})^T$ (resp. $(\Theta^*_{11}, \dots, \Theta^*_{nn})^T$) is a right eigenvector of Γ (resp. Θ) associated with the zero eigenvalue. Here, Γ^*_{ii} (resp. Θ^*_{ii}) is the cofactor of the ith diagonal entry of Γ (resp. Theta), and $sgn(\Gamma^*_{ii}) = (-1)^{n-1}$ (resp. $sgn(\Theta^*_{ii}) = (-1)^{n-1}$). Assuming that the matrix Γ (resp. Θ) is irreducible, we have that $(-1)^{n-1}(\Gamma^*_{11}, \dots, \Gamma^*_{nn})^T$ (resp. $(-1)^{n-1}(\Theta^*_{11}, \dots, \Theta^*_{nn})^T$) is strictly positive, *i.e.*, $\delta_i = (-1)^{n-1}\Gamma^*_{ii} > 0$ (resp. $\xi_i = (-1)^{n-1}\Theta^*_{ii} > 0$) for all i. Therefore, we have explicit formulas for the components of the vector δ (resp. ξ) in terms of the coefficients of Γ (resp. Θ) at our disposal. For two patches, we have $\delta = (\gamma_{12}, \gamma_{21})^T$ (resp. $\xi = (\theta_{12}, \theta_{21})^T$), and for three patches, we have $\delta = (\delta_1, \delta_2, \delta_3)^T$ (resp. $\xi = (\xi_1, \xi_2, \xi_3)^T$), where

$$\begin{cases} \delta_1 = \gamma_{12}\gamma_{13} + \gamma_{12}\gamma_{23} + \gamma_{32}\gamma_{13}, \\ \delta_2 = \gamma_{21}\gamma_{13} + \gamma_{21}\gamma_{23} + \gamma_{31}\gamma_{23}, \\ \delta_3 = \gamma_{21}\gamma_{32} + \gamma_{31}\gamma_{12} + \gamma_{31}\gamma_{32}. \end{cases} \quad \text{resp.} \quad \begin{cases} \xi_1 = \theta_{12}\theta_{13} + \theta_{12}\theta_{23} + \theta_{32}\theta_{13}, \\ \xi_2 = \theta_{21}\theta_{13} + \theta_{21}\theta_{23} + \theta_{31}\theta_{23}, \\ \xi_3 = \theta_{21}\theta_{32} + \theta_{31}\theta_{12} + \theta_{31}\theta_{32}. \end{cases} \tag{A.1}$$

In Lemma 2.1 of Guo *et al.* [49], explicit formulas for the components of the vector δ (resp. ξ) are given with respect to the coefficients of Γ (resp. Θ) as follows:

$$\delta_k = \sum_{T\in\mathscr{T}_k} \prod_{(i,j)\in E(T)} \gamma_{ij} \quad \text{resp. } \xi_k = \sum_{T\in\mathscr{T}_k} \prod_{(i,j)\in E(T)} \theta_{ij}, \qquad k = 1, \dots, n, \tag{A.2}$$

where $\mathscr{T}_k$ is the set of all directed trees of n vertices rooted at the kth vertex, and $E(T)$ denotes the set of arcs in a directed tree T.

The matrix Γ (resp. Θ) being irreducible means that the set of the source and sink patches cannot be partitioned into two nonempty disjoint subsets, I and J, such that there is no migrations between a patch in subset I and a patch in subset J, i.e the irreducibility of matrix Γ (resp. Θ) implies that every patch in the model (3.3) is connected by migration term, *i.e.* the species can reach any ith patch from any j-patch. For Two-patch model, the matrix Γ (resp. Θ) is irreducible if and only if γ_{12} and γ_{21} (resp. θ_{12} and θ_{21}) are positives. If $n = 3$, we have five cases, see Figure A.1.

We recall Lemma B.1 of Elbetch *et al.* [2]:

Lemma A.1. *The matrices $\mathscr{L}_1$ and $\mathscr{L}_2$ defined by (4.7) are stable, that is to say, all its eigenvalues have negative real part.*

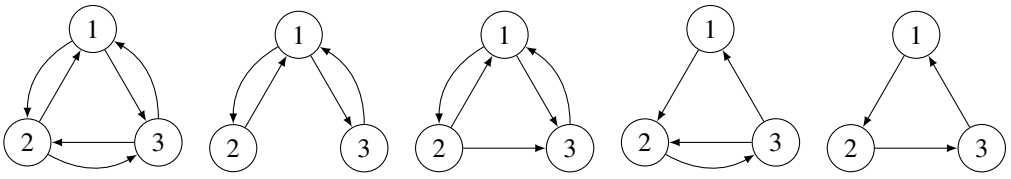

FIGURE A.1. The assumption that the matrix Γ (resp. Θ) is irreducible, implies that the species can reach any ith patch from any j-patch. For Three-patch model, under the irreducibility hypothesis on the matrix Γ (resp. Θ), there are five possible cases, modulo permutation of the three patches. The two graphs $\mathscr{G}_1$ and $\mathscr{G}_2$ for which the migration matrix may be symmetric, if $\gamma_{ij} = \gamma_{ji}$ (resp. $\theta_{ij} = \theta_{ji}$). For the remaining cases, the graphs $\mathscr{G}_3, \mathscr{G}_4$ and $\mathscr{G}_5$, cannot be symmetrical.

Proof. We consider the two matrices

$$G_k := \begin{bmatrix} & L_k - U_k & & V_k \\ 0 & \dots & 0 & 0 \end{bmatrix}, \qquad P := \begin{bmatrix} & I & & 0 \\ 1 & \dots & 1 & 1 \end{bmatrix},$$

where L_k, V_k, and U_k are defined right after (4.7). We prove that the two matrices Γ (resp. Θ) and G_1 (resp. G_2) are conjugate by the matrix P, that is to say $P^{-1}G_1P = \Gamma$. (resp. $P^{-1}G_2P = \Theta$.)
The inverse of matrix P is given by

$$P^{-1} = \begin{bmatrix} & I & & 0 \\ -1 & \dots & -1 & 1 \end{bmatrix}.$$

We have

$$P^{-1}G_1P = \begin{bmatrix} & L_1 & & V_1 \\ \gamma_{n1} & \dots & \gamma_{nn-1} & -\sum_{j=1, j\neq 1}^{n} \gamma_{jn} \end{bmatrix} = \Gamma.$$

Two conjugate matrices have the same eigenvalues. As the matrix G_1 is block-triangular, its eigenvalues are zero and the eigenvalues of the matrix $L_1 - U_1$. Therefore, since 0 is an simple eigenvalue of the matrix Γ, the eigenvalues of the matrix $L_1 - U_1$ are the eigenvalues of the matrix Γ except 0. All non-zero eigenvalues of Γ have negative real part which prove that the matrix $\mathscr{L}_1$ is stable. By the same method we prove that $\mathscr{L}_2$ is stable. □